

Final Report
MOST beamline@Elettra 2.0 – optical layout
Latest results, decisions and updates

Roberta TOTANI
IOM-CNR
34149 Basovizza, Italy

Altri autori:
Marcello CORENO, ISM-CNR, Luca POLETTO IFN-CNR, Fabio FRASSETTO, IFN-
CNR, Anna BIANCO Sincrotrone Trieste, Monica DE SIMONE IOM-CNR

December 2020

Per presa visione:

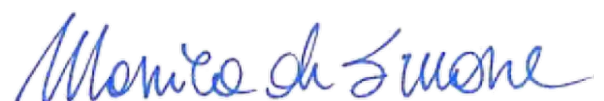


TABLE OF CONTENTS

1. INTRODUCTION	3
2. SOURCES	5
2.1. Low-Energy Undulator (LEU), 8 eV - 200 eV	5
2.2. High Energy Undulator (HEU)	6
<i>a. ELETTRA @ 2 GeV.....</i>	<i>7</i>
<i>b. ELETTRA @ 2.4 GeV.....</i>	<i>12</i>
<i>c. ELETTRA 2.0 @ 2.4 GeV.....</i>	<i>15</i>
3. THERMAL LOAD EVALUATION ON THE FIRST OPTICAL ELEMENT	21
4. MOST PRELIMINARY OPTICAL DESIGN - INTERMEDIATE AND HIGH ENERGY	31
5. MOST BEAMLINE: A STEP-BY-STEP REALIZATION	38
REFERENCES	40

1. INTRODUCTION

The design and the realization of the new MOST (MOlecular Science&Technology) beamline are part of the storage ring and beamline upgrade that will lead to a completely renewed ELETTRA, in the context of the project known as ELETTRA 2.0. The MOST beamline will take the place of the already existing Gas Phase Photoemission (GasPhase) and Circular Polarization (CiPo) beamlines. It will be dedicated to:

- Atomic and molecular physics
- Astrophysics and astrochemistry
- Plasma and materials physics
- Electron dynamics

These investigations will be performed by means of:

- Photoabsorption
- Photoemission
- Mass Spectrometry
- Dichroic spectroscopies
- Time-resolved spectroscopies, by means of synchrotron radiation and a femtosecond solid-state laser.

MOST will be designed to provide the highest possible performances with the current light source and to take full advantage of the improved ELETTRA 2.0, thanks to the employment of state-of-the-art optical technologies.

The main requirements that MOST will have to fulfill and that are driving its design are:

- Higher flux in a wider photon energy range (from 8 - 10 eV, up to 3000 eV)
- High resolution
- High spectral purity, with a total rejection of higher order content
- Full polarization control.

In this final report the latest results obtained from the high-energy undulator characterization and from the optical elements thermal load evaluation are displayed. Besides, a preliminary design of the optical layout for the intermediate/high photon energy range and a discussion about MOST realization steps and on its whole optical layout including the low-energy optical elements are also included.

2. SOURCES

The beamline will receive light by two brand-new undulators, one for the low photon energy range (8 eV - 200 eV) and one for the intermediate/high photon energy range (80 eV - 3000 eV).

2.1. Low-Energy Undulator (LEU), 8 eV - 200 eV

The LEU will have a period length of 132 mm and 18 periods. It is going to operate with a fixed gap and a variable phase. In this way, a more compact design and a cheaper mechanics and control system will be allowed, guaranteeing the same functionalities of a conventional variable gap undulator.

The maximum values of the deflection parameter K for the horizontal, vertical and helical polarization, together with the corresponding lowest reachable photon energies, are reported in Table 1, for the case of ELETTRA 2.0, operated at 2 GeV [1].

Polarization	K_{\max}	E_{\min} (eV)@2 GeV
Horizontal	$K_y=5.1$	20
Vertical	$K_x=8$	8
Circular	$K_h=4.3$	15

Table 1. ELETTRA 2.0, 2 GeV. Maximum values of the deflection parameter K for the different light polarization and corresponding lowest photon energy values.

The estimated photon flux in circular polarization and in linear polarization for the first three harmonics is shown in [Figure 1](#), as a function of the photon energy, for the case of ELETTRA 2.0 operated at 2 GeV [1].

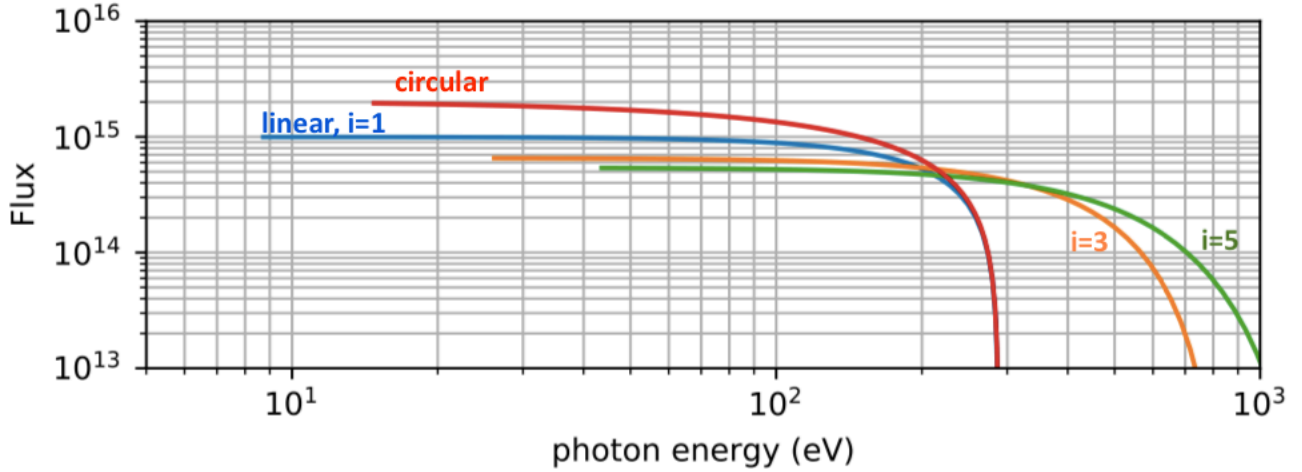


Figure 1. ELETTRA 2.0, 2 GeV. LEU provided flux, as a function of the photon energy, in circular and linear polarization and, in the latter case, for the 1st, 2nd and 3rd harmonic [1].

2.2. High Energy Undulator (HEU)

The high-energy undulator (HEU) is an Elliptical Polarization Undulator (EPU), with a period of 50.36 mm and 28 periods, whose main parameters as summarized in Table 2 for ELETTRA 2.0 operated at 2 GeV and 2.4 GeV².

Polarization	B_{\max} (T)	K_{\max}	E_{\min} (eV) @2 GeV	E_{\min} (eV) @2.4 GeV
Horizontal	$B_y=0.85$	$K_y=4.0$	83.9	120.8
Vertical	$B_x=0.62$	$K_x=2.91$	143.7	206.9
Circular	$B_x= B_y=0.51$	$K_x=K_y=2.4$ $K_{\text{comp}}=3.39$	111.7	160.9

Table 2: MOST High-energy EPU main parameters. The lowest photon energy is provided in horizontal linear polarization, which is the geometry allowing the highest value of the deflection parameter K .

Hereafter, the source characterization for ELETTRA operated at 2 GeV and 2.4 GeV and ELETTRA 2.0 operated at 2.4 GeV, is reported. These results have been obtained by Anna

Bianco (Elettra Sincrotrone Trieste) by means of the Spectra software [3] using, as machine input parameters:

- E = storage ring energy
- I = storage ring current
- ϵ_z, ϵ_x = vertical and horizontal electron emittance, respectively
- Coupling = ϵ_z/ϵ_x
- Energy spread of the electron beam.

And as long straight section parameters:

- β_x, β_y = betatron function parameters
- α_x, α_y = parameters of the lattice function, to denote the slope of the phase ellipse of the electron beam
- $\eta_x, \eta_y, \eta_x', \eta_y'$ = dispersion function parameters in meters (η_x, η_y) and radians (η_x', η_y')

Let us examine the three different situations.

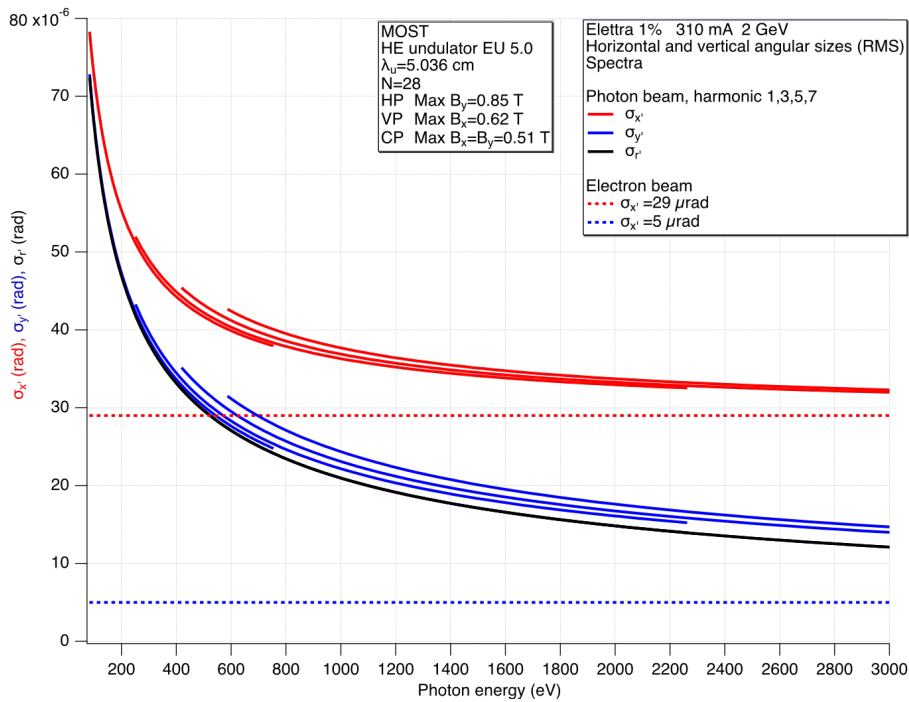
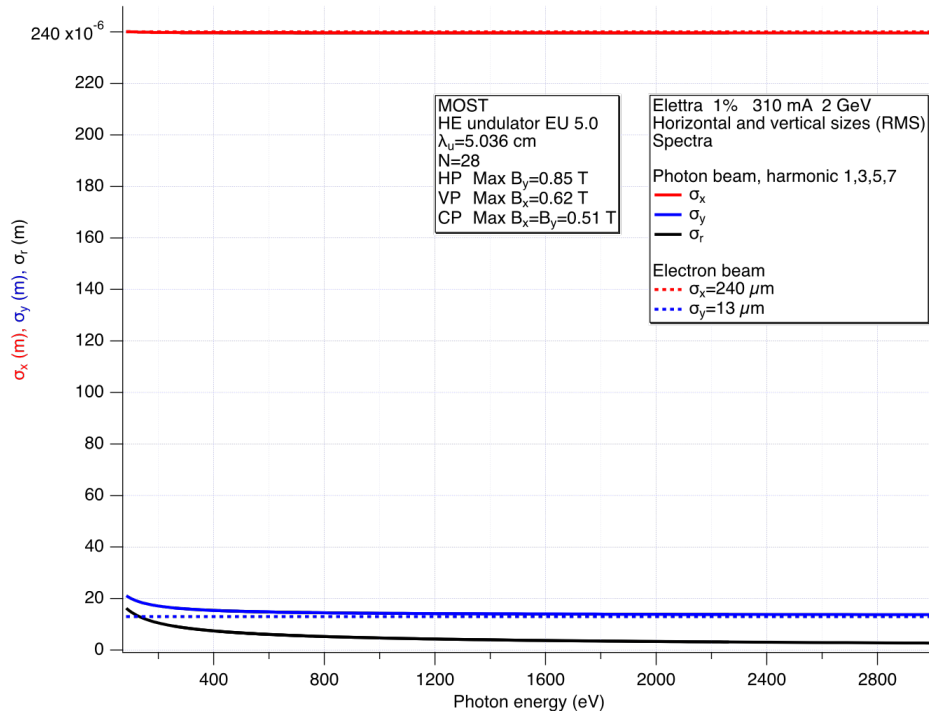
a. ELETTRA @ 2 GeV

E (GeV)	I (A)	Coupling (%)	Coupling (%)	ϵ_z (pm rad)	Energy spread (%)
2.0	0.31	1	7000	70	0.078

Table 3. Machine parameters

β_x (m)	β_y (m)	α_x	α_y	η_x (m)	η_y (m)	η_x'	η_y'
8.2	2.6	0	0	0	0	0	0

Table 4. Long-straight section parameters.



[Back](#) to Fig.8
[Back](#) to Fig.14

Figure 2. Horizontal (x) and vertical (y) RMS spatial ([top](#)) and angular ([bottom](#)) photon beam size (σ) for harmonics 1, 3, 5, and 7. The angular values are indicated by adding a prime ($'$). The case of the filament beam, i.e. the ideal zero-emittance electron beam, is also reported (σ_r and σ_r'). For comparison, the electron beam sizes are also shown (dashed lines). They clearly indicate the influence of the electron beam on the spatial dimensions of the photon beam. Differently, the angular dimensions depend on the energy spread, which increases with the harmonic number.

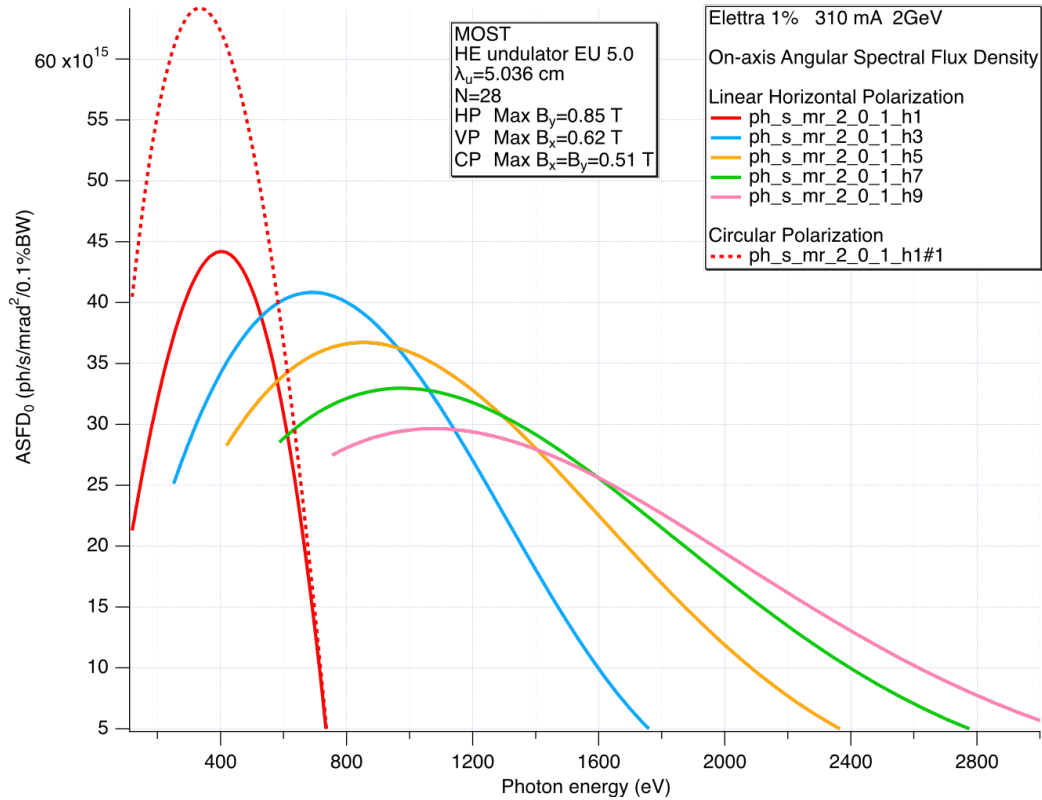
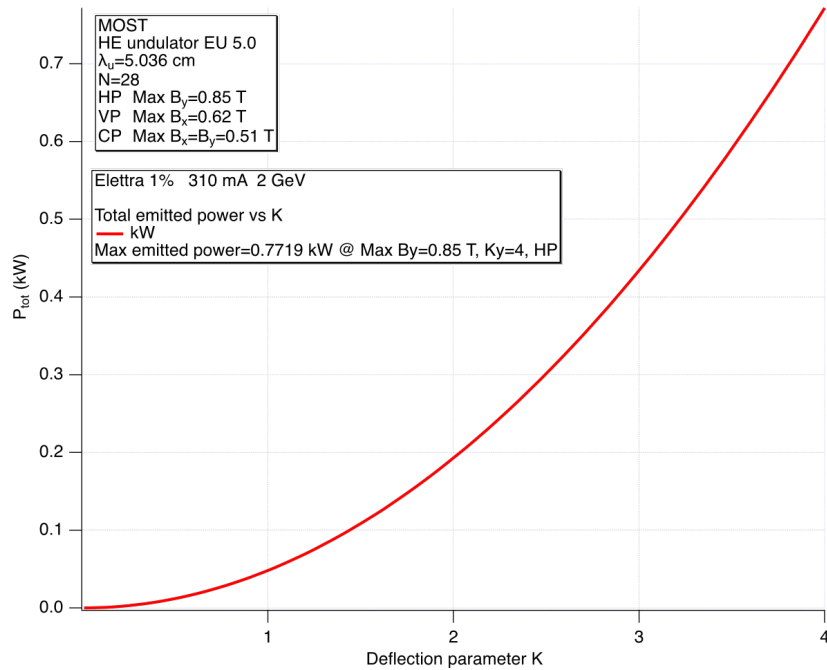


Figure 3. On-axis Angular Spectral Flux Density at zero emittance ($ASFD_0$) for linear horizontal (harmonics from 1 to 9) and circular polarization. $ASFD_0$, measured in photons/s/mrad²/0.1% of the bandwidth (BW), represents the flux density in the energy space, along the photon beam axis.



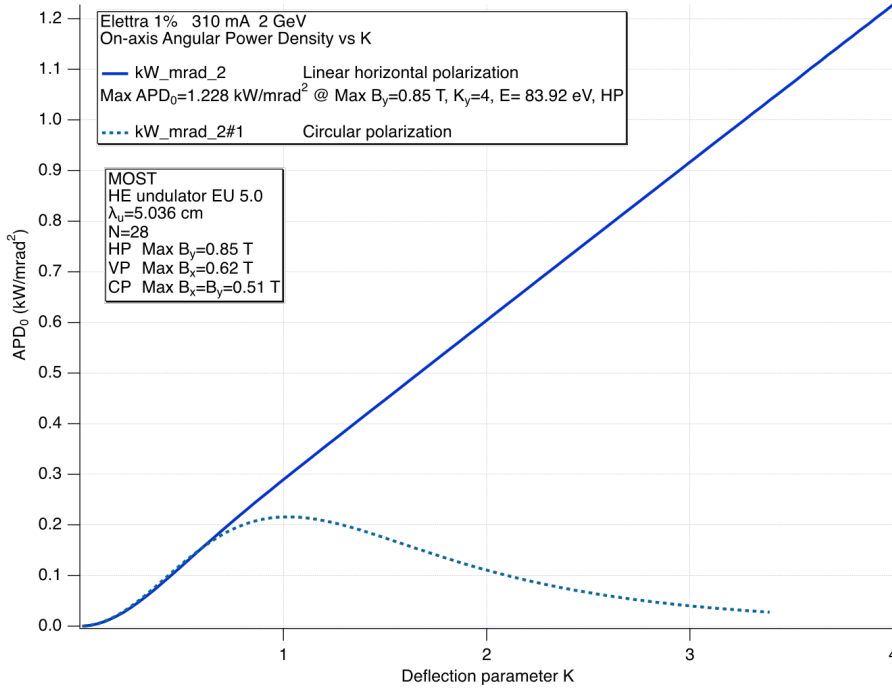
[Back to Fig.6](#)

Figure 4. Total emitted power P_{tot} as a function of the deflection parameter K . P_{tot} depends neither on the electron beam emittance, nor on the light polarization. Indeed, it is given by the analytical expression [4]:

$$P_{tot}[W] = 7.257 \frac{E^2[GeV]K^2NI[A]}{\lambda_u[cm]} \quad (1)$$

[Back to Fig.10](#)
[Back to Fig.16](#)

Where E is the storage ring energy and λ_u and N are the undulator period length and number of periods, respectively. In particular, it depends on K^2 , as clearly visible from the parabola represented in [Figure 4](#).



[Back to Fig.6](#)

Figure 5. On-axis Angular Power Density (APD) as a function of K, for linear horizontal (solid line) and circular polarization (dashed line). In horizontal linear polarization, the K-dependence and the I-dependence are linear in first approximation, as explained from the analytical relationship at zero emittance [3]:

$$APD_0 \left[\frac{W}{mrad^2} \right] = 10.84 B[T] E^4[GeV] NI[A] G(K) \quad (2)$$

[Back to Fig.11](#)
[Back to Fig.17](#)

Where $G(K) \approx 1$ for $K > 0.8$.

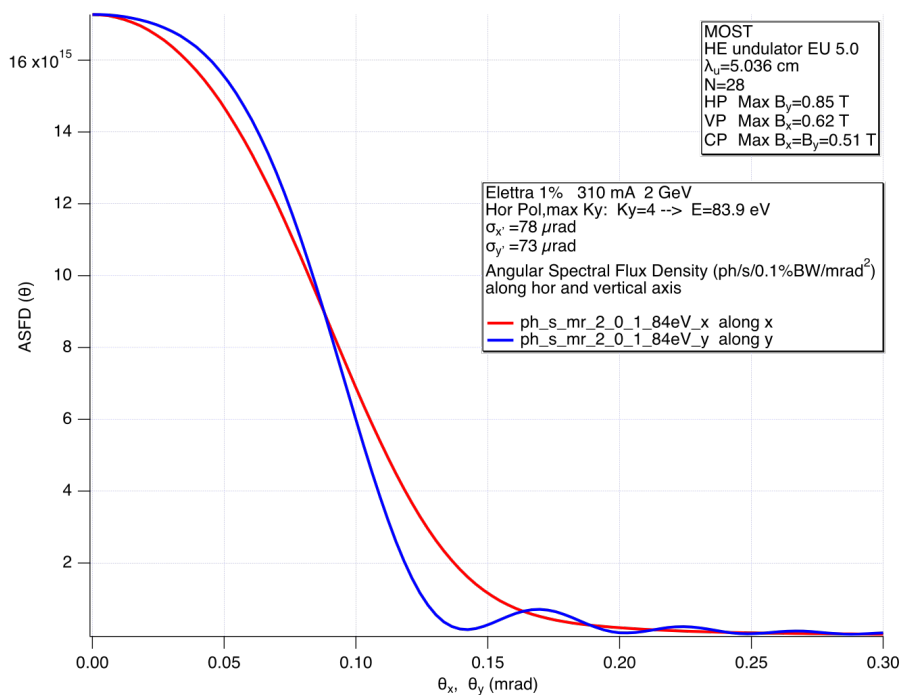


Figure 6. ASFD along the horizontal and vertical axis, evaluated in linear horizontal polarization, considering the maximum value of the deflection parameter ($K_y = 4$) and a first harmonic energy of 83.9 eV. This is indeed the most critical situation for the HEU, because is characterized by the highest P_{tot} and the highest on-axis APD_0 .

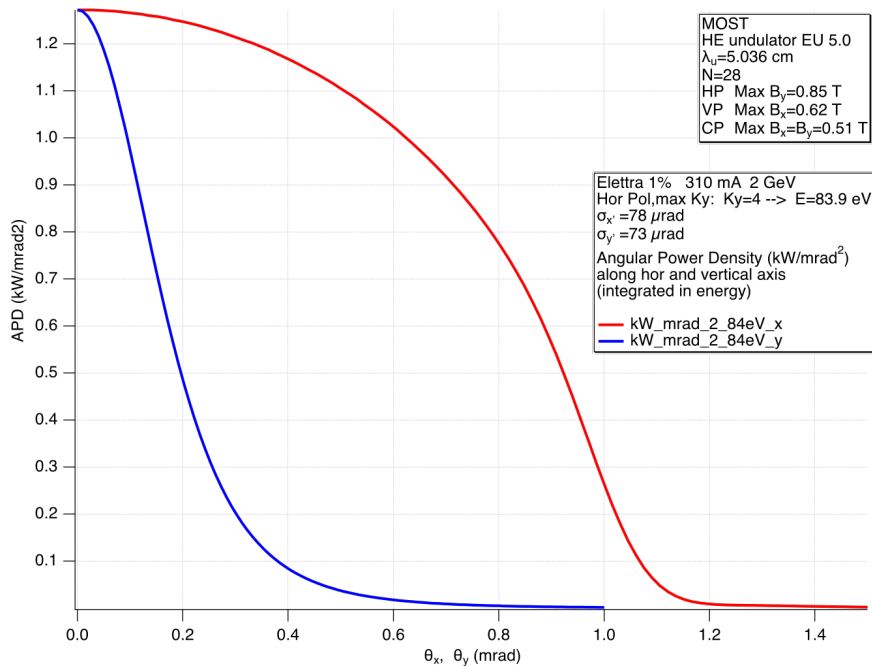


Figure 7. APD along the horizontal and vertical axis, in linear horizontal polarization ($K_y = 4$, 83.9 eV).

b. ELETTRA @ 2.4 GeV

E (GeV)	I (A)	Coupling (%)	ϵ_x ($\mu\text{m rad}$)	ϵ_z ($\mu\text{m rad}$)	Energy spread (%)
2.0	0.160	1	10000	100	0.095

Table 5. Machine parameters

β_x (m)	β_y (m)	α_x	α_y	η_x (m)	η_y (m)	$\eta_{x'}$	$\eta_{y'}$
8.2	2.6	0	0	0	0	0	0

Table 6. Long straight section parameters

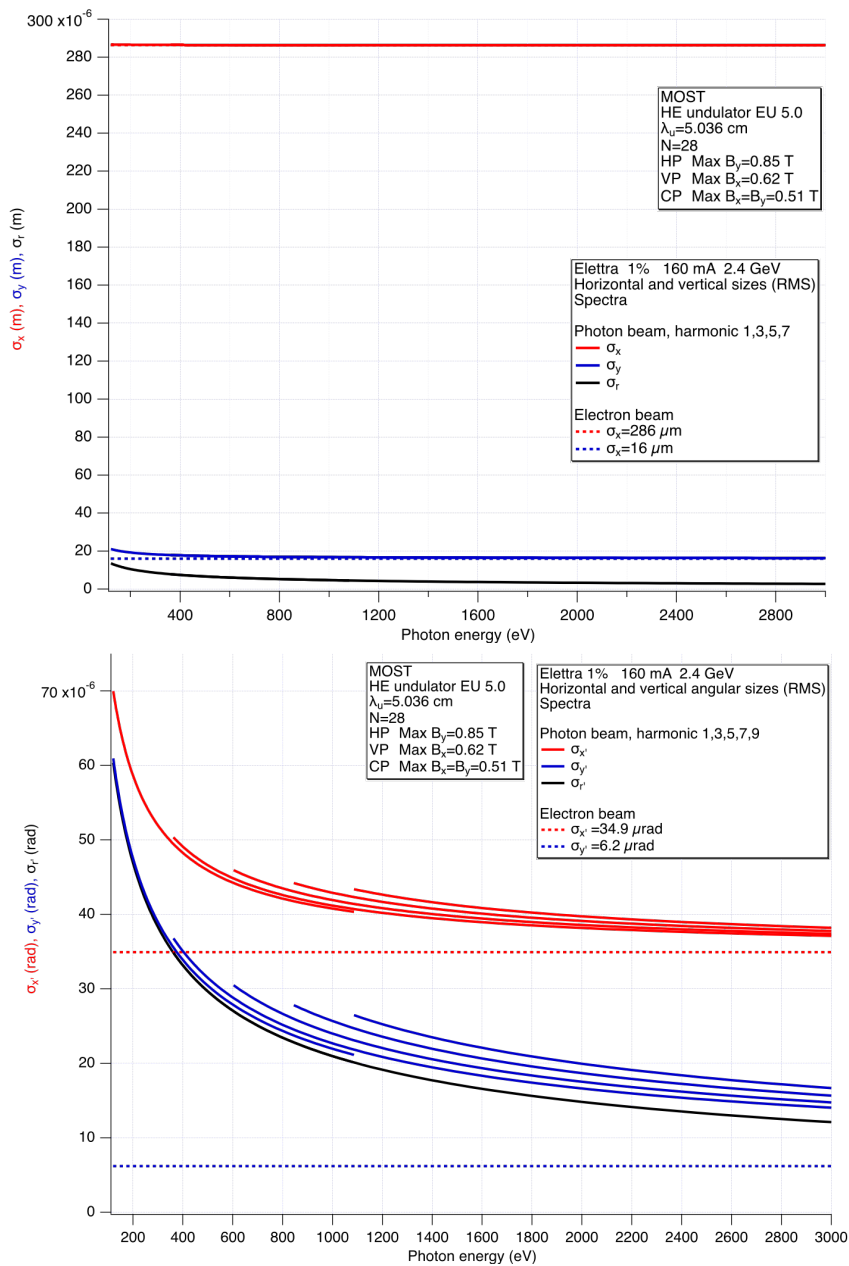


Figure 8. Photon beam spatial ([top](#)) and angular ([bottom](#)) RMS sizes. Parameters and symbols as for [Fig.2](#).

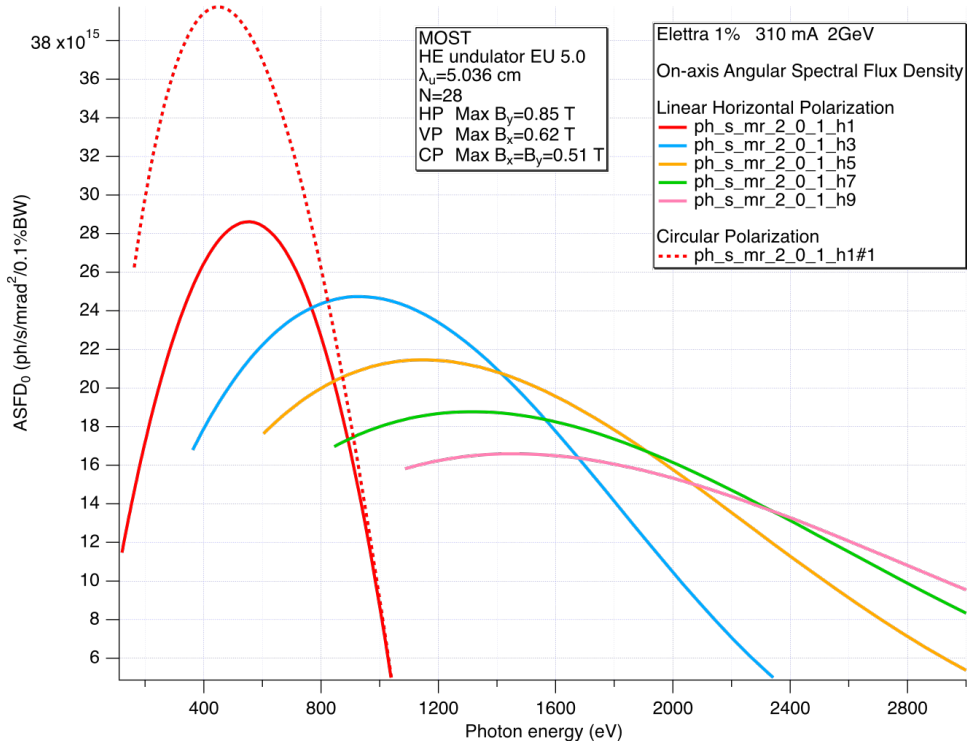


Figure 9. On-axis ASFD at zero emittance (ASFD₀) for linear horizontal (harmonics from 1 to 9) and circular polarization.

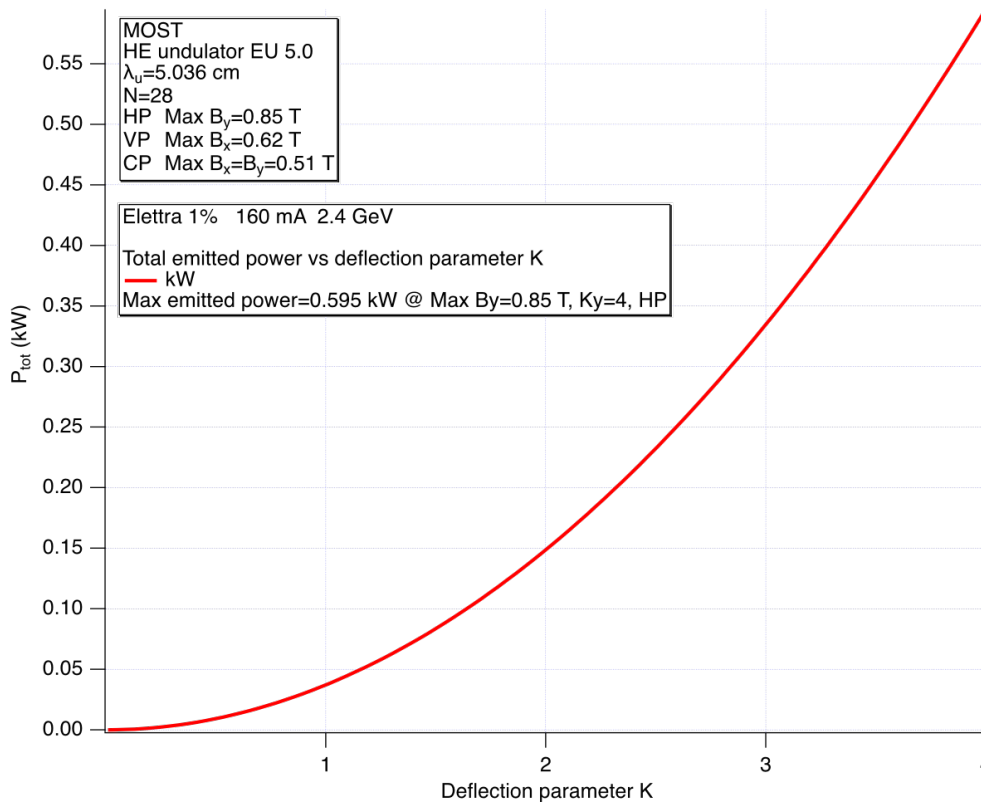
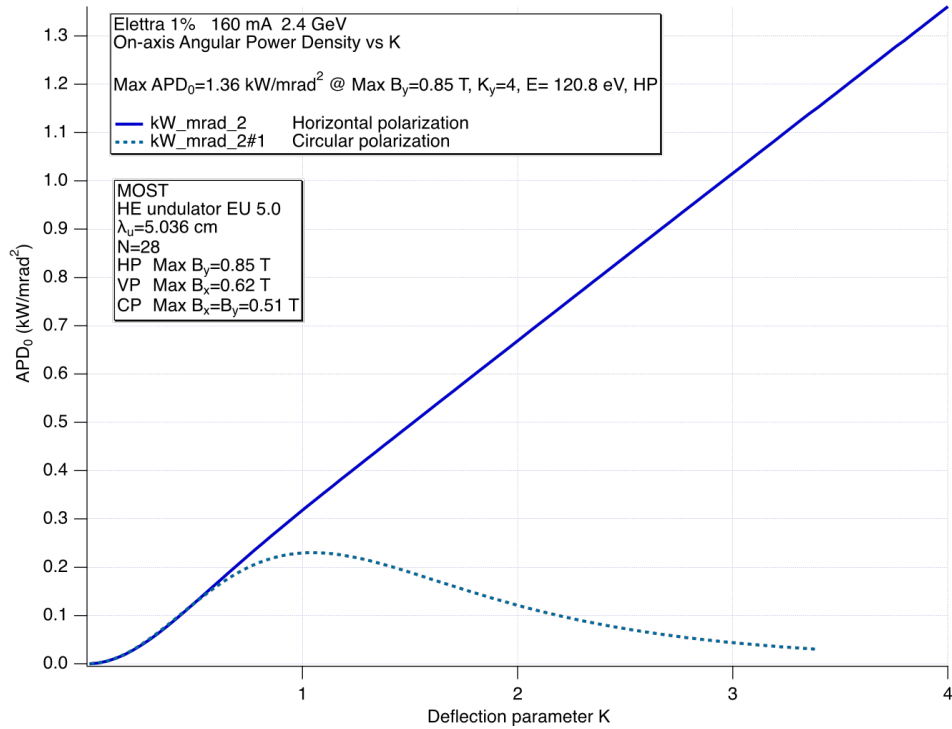


Figure 10. P_{tot} (Eq.1) as a function of the deflection parameter K.

[Back to Fig.12](#)



[Back to Fig.12](#)

Figure 11. On-axis APD (Eq.2) as a function of K, for linear horizontal (solid line) and circular polarization (dashed line).

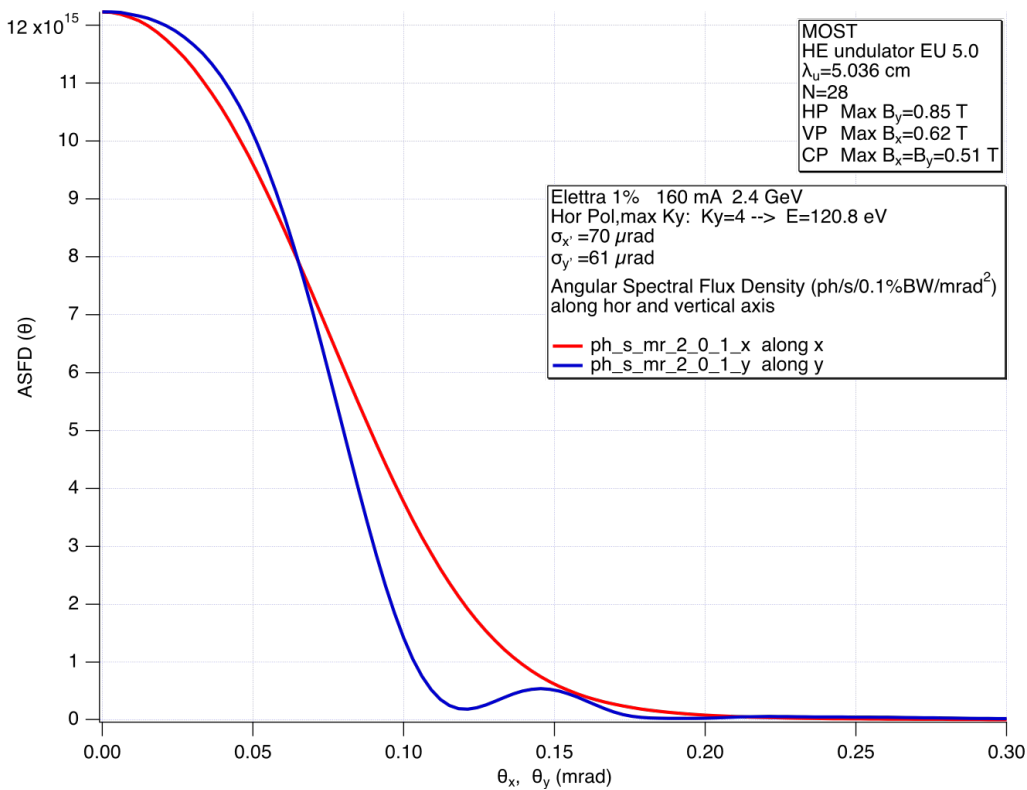


Figure 12. ASFD along the horizontal and vertical axis, evaluated in linear horizontal polarization, considering the maximum value of the deflection parameter ($K_y = 4$) and a first harmonic energy of 120.8 eV. This is indeed the most critical situation for the HEU, because this geometry is characterized by the highest P_{tot} and the highest on-axis APD.

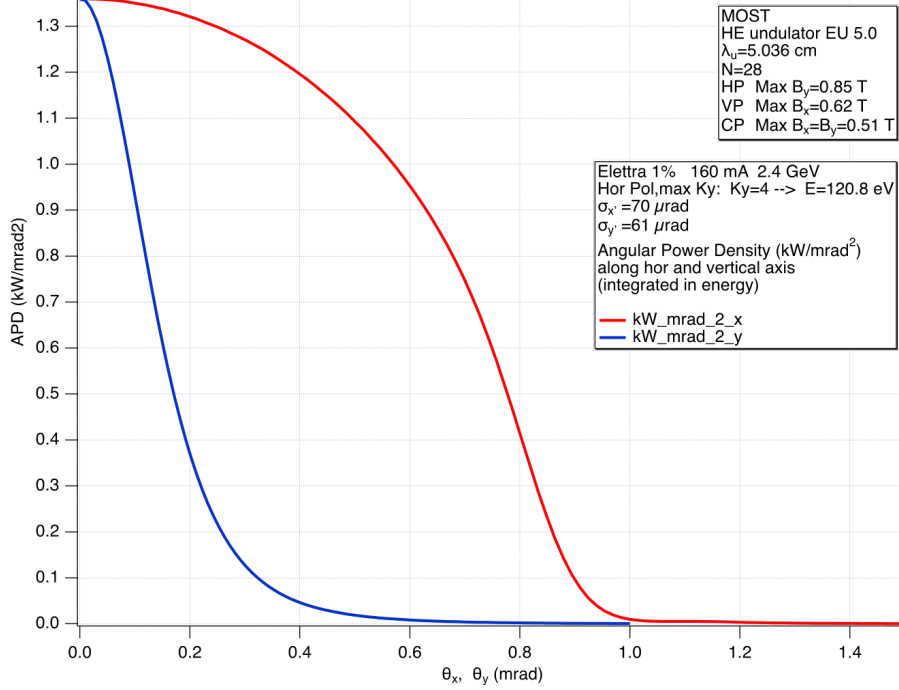


Figure 13. APD along the horizontal and vertical axis, for the linear horizontal polarization ($K_y=4$, 120.8 eV).

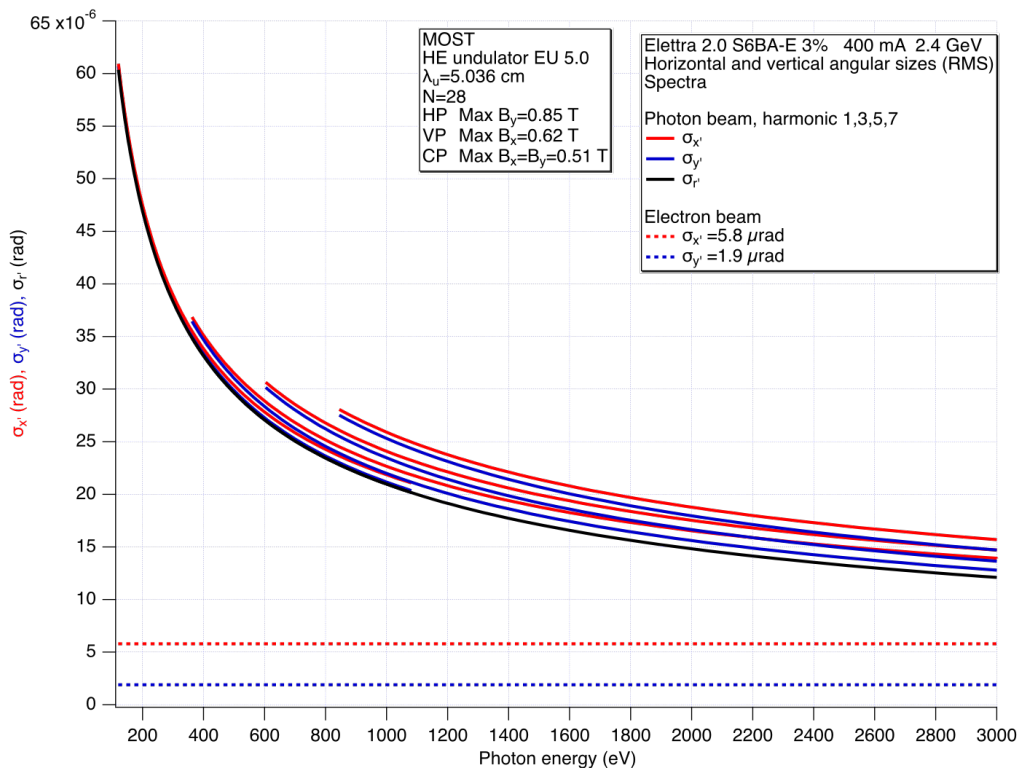
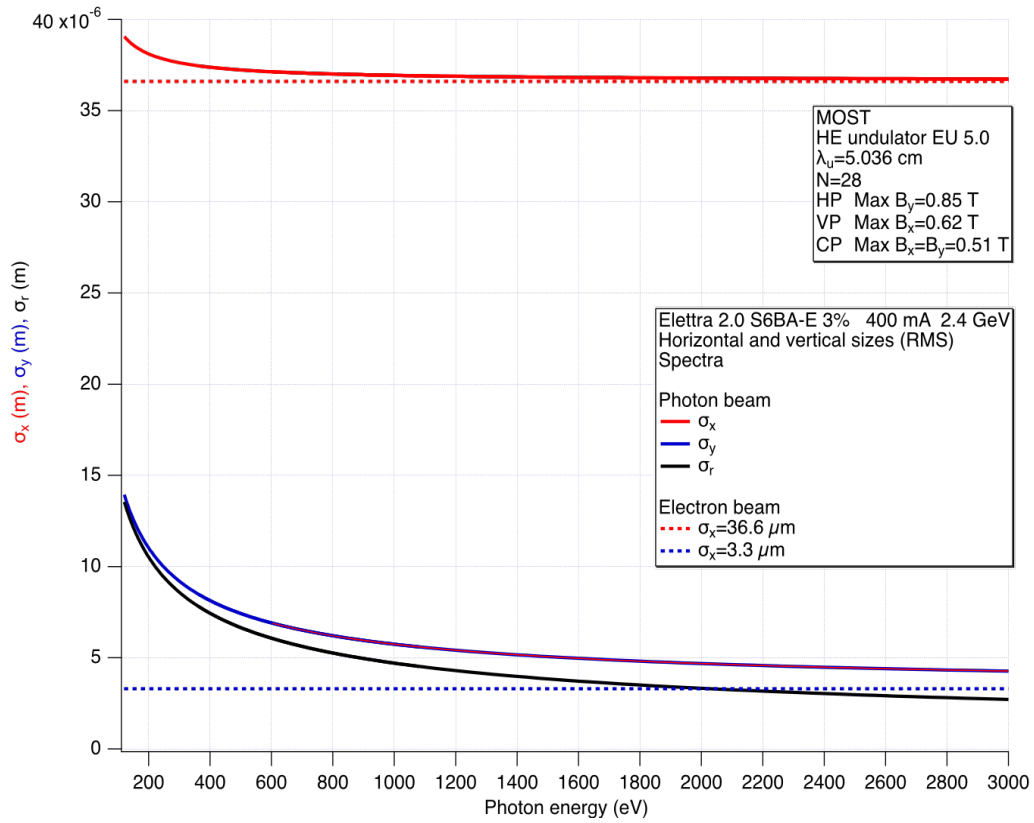
c. ELETTRA 2.0 @ 2.4 GeV

E (GeV)	I (A)	Coupling (%)	ϵ_x (pm rad)	ϵ_z (pm rad)	Energy spread (%)
2.4	0.4	3	213	6.4	0.0997

Table 7. Machine parameters

β_x (m)	β_y (m)	α_x	α_y	η_x (m)	η_y (m)	$\eta_{x'}$	$\eta_{y'}$
6.3	1.7	0	0	0	0	0	0

Table 8. Long straight section parameters.



[Back to text](#)

Figure 14. Photon beam spatial ([top](#)) and angular ([bottom](#)) RMS sizes. Parameters and symbols as for [Fig.2](#).

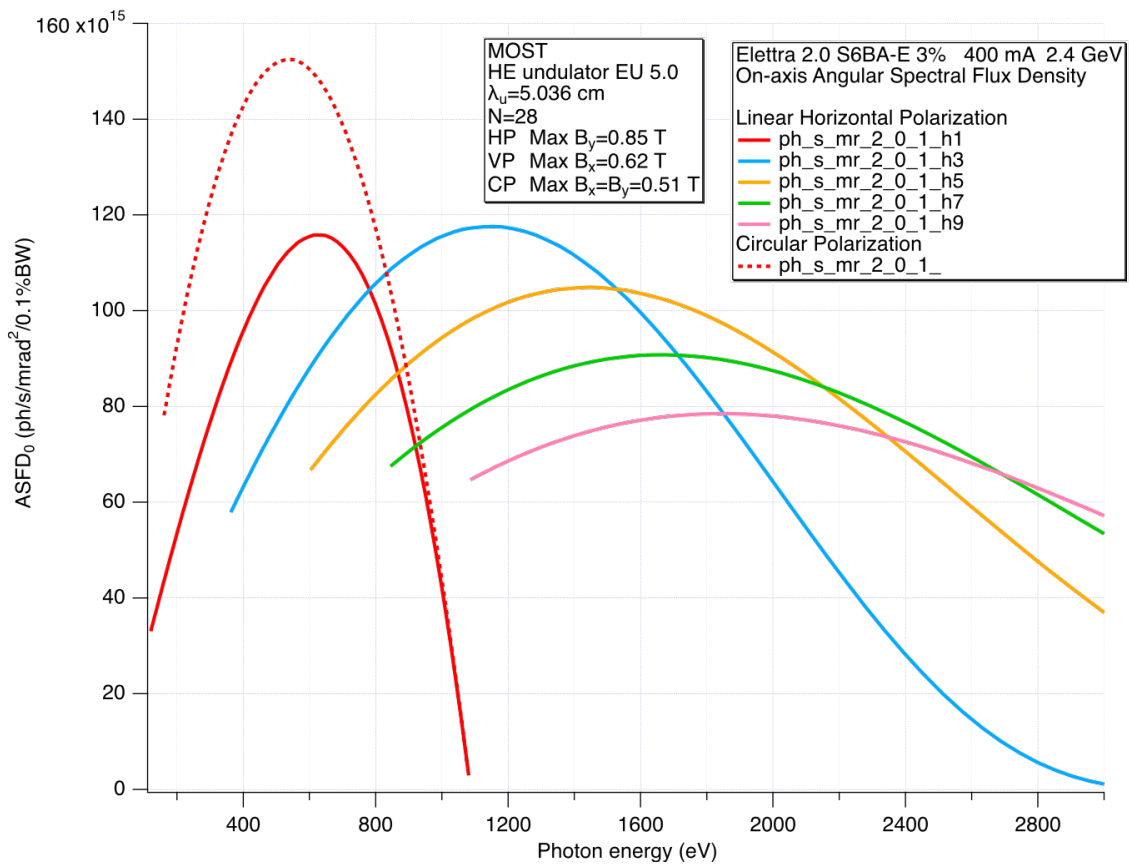
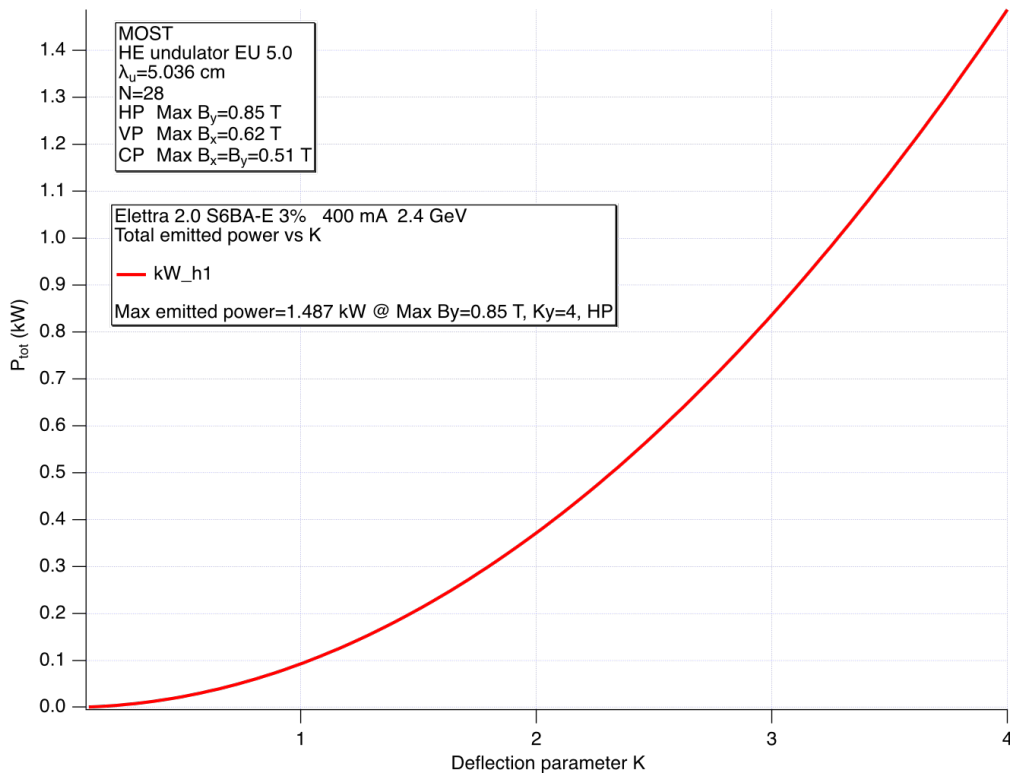
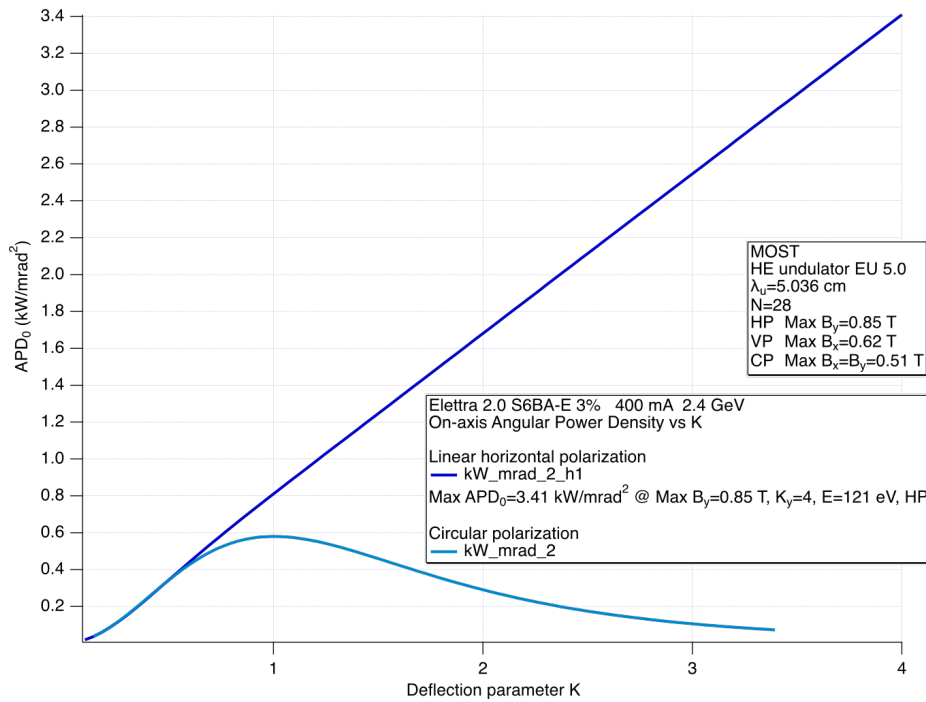


Figure 15. On-axis $ASFD_0$ for linear horizontal (harmonics from 1 to 9) and circular polarization.



[Back to Fig.18](#)

Figure 16. P_{tot} (Eq.1) as a function of the deflection parameter K.



[Back to Fig.18](#)

Figure 17. On-axis APD (Eq.2) as a function of K, for linear horizontal and circular polarization dashed line.

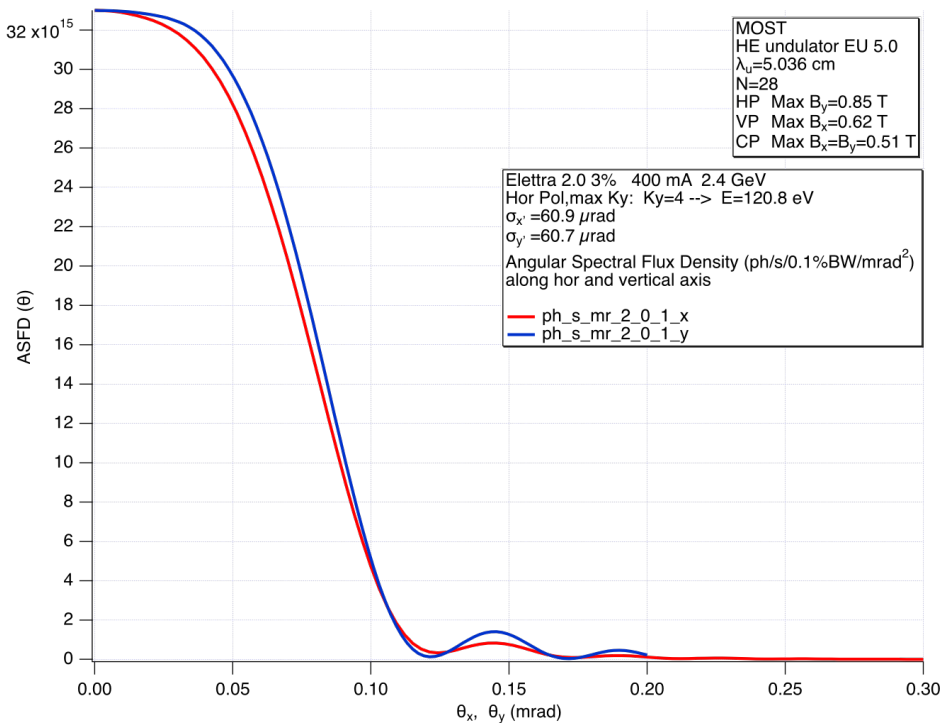


Figure 18. ASFD along the horizontal and vertical axis, evaluated in linear horizontal polarization, considering the maximum value of the deflection parameter ($K_y = 4$) and a first harmonic energy of 120.8 eV. This is the most critical situation for the HEU, because this geometry is characterized by the highest P_{tot} and the highest on-axis APD.

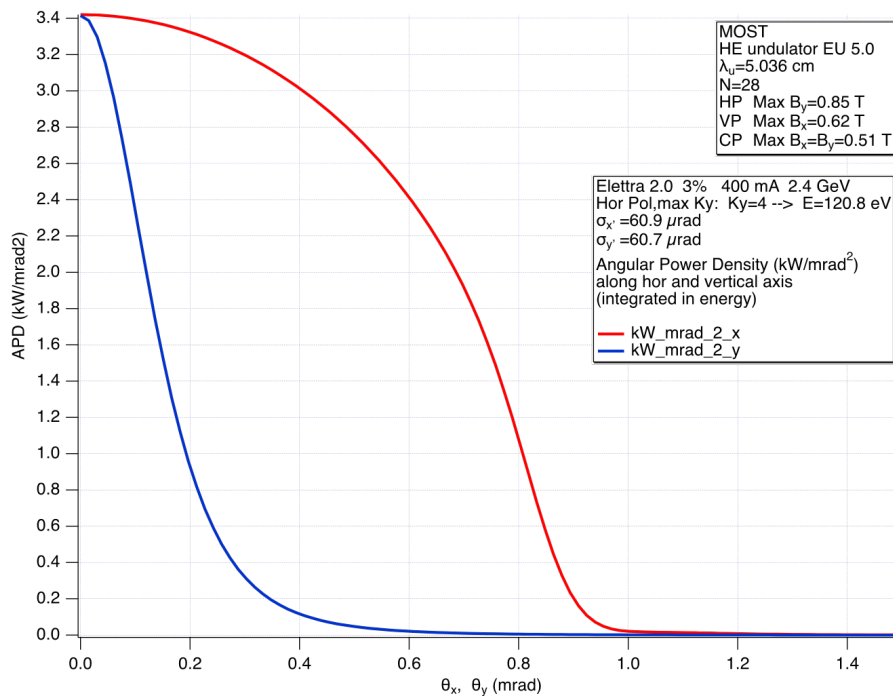


Figure 19. APD along the horizontal and vertical axis, for the linear horizontal polarization ($K_y=4$, 120.8 eV).

For this case, the APD contour plot has been evaluated and is displayed in [Figure 20](#).

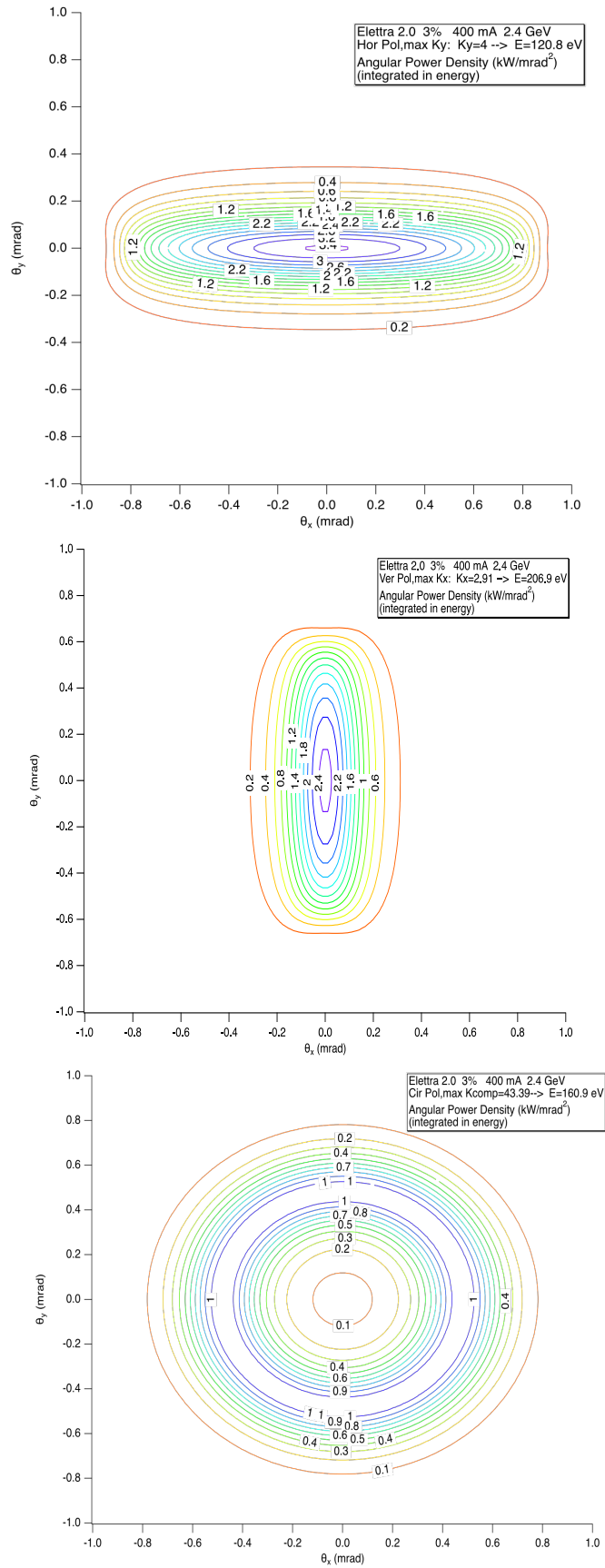


Figure 20. APD Contour plot for the case of Kmax in horizontal polarization ([top](#)), vertical polarization ([center](#)) and circular polarization (CP, [bottom](#)). The first harmonic energies are, for the three polarization configuration respectively, 121 eV, 207 eV and 161 eV.

3. THERMAL LOAD EVALUATION ON THE FIRST OPTICAL ELEMENT

ELETTRA 2.0 will provide higher P_{tot} than the current ELETTRA values (see table 9).

Therefore, an evaluation of the thermal load on the optical elements of the future beamlines is of paramount importance in order to take into account possible deformations and to realize a correct design of the necessary cooling systems.

	Elettra 2 GeV 310 mA	Elettra 2.4 GeV 160 mA	Elettra 2.0, 2.4 GeV 400 mA
P_{tot} (kW)	772	595	1390 (x 2.3)

Table 9. Comparison among the emitted P_{tot} for ELETTRA (2 GeV, 2.4 GeV) and ELETTRA 2.0 (2.4 GeV).

A calculation of the power absorbed by the front-end slits of the machine, of the power arriving on the first mirror and of the power subsequently absorbed and then reflected on the second mirror has been realized for the most critical case of ELETTRA 2.0 operated at 2.4 GeV. As seen above, this occurs in linear horizontal polarization, with $K_y=4$ and a first harmonic energy of 120.8 eV, i.e. in the geometry that maximizes both P_{tot} and APD_0 .

We supposed to open the front-end double slit, situated at 11.48 m from the center of the straight section, in order to accept 4σ in both the horizontal and the vertical direction. As σ_x and σ_y at $K_y=4$ and 120.8 eV are, respectively, 60.9 μrad and 60.7 μrad (see [Fig.14](#)), we accepted roughly 0.24 mrad in both directions. Knowing the Spectral Flux Density (SFD), defined as the photons/s/mrad²/0.1%BW, the emitted P_{tot} is obtained by evaluating the integral

$$P_{\text{tot}} = 1000 \int F(E) dE \quad (3) \quad \text{Back to text}$$

on a range of photon energies ranging, ideally, from 0 to ∞ .

With the help of the Spectra software [2], we evaluated the SFD before and after the front-end exit slit and, by integrating, we obtained the relative P_{tot} . In this way we evaluated that 1.39 kW will be delivered by the source on the slits, 144 W will arrive on the first mirror and, consequently, 1.25 kW will be absorbed by the slits. [Fig.21](#) shows the SFD before the front-end exit slit.

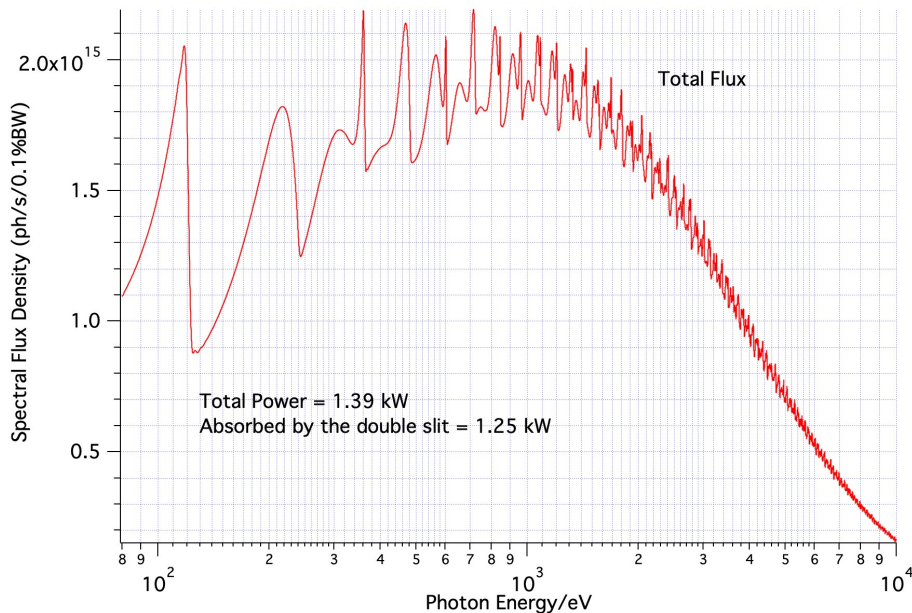
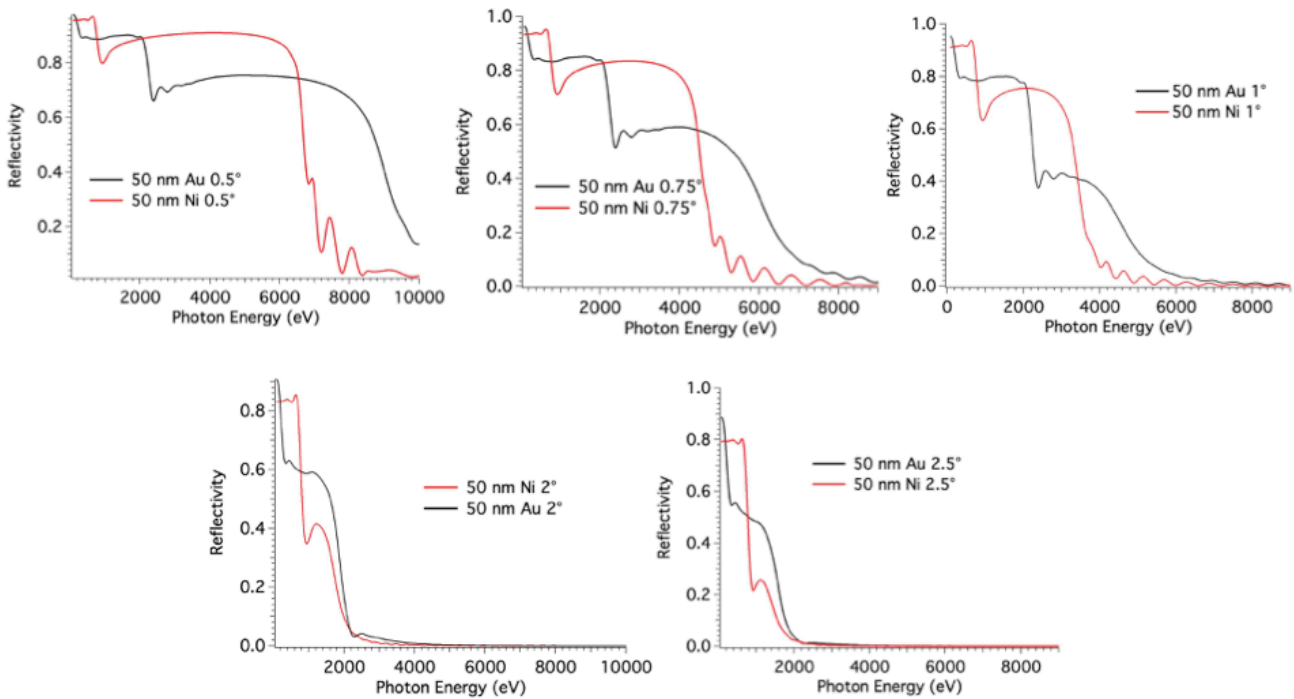


Figure 21. SFD before the front-end exit slit.

The calculation of the absorbed and the reflected power on the first mirror has been realized considering several incident angles: 0.5°, 0.75°, 1°, 2° and 2.5°. Both Au-coated and Ni-coated

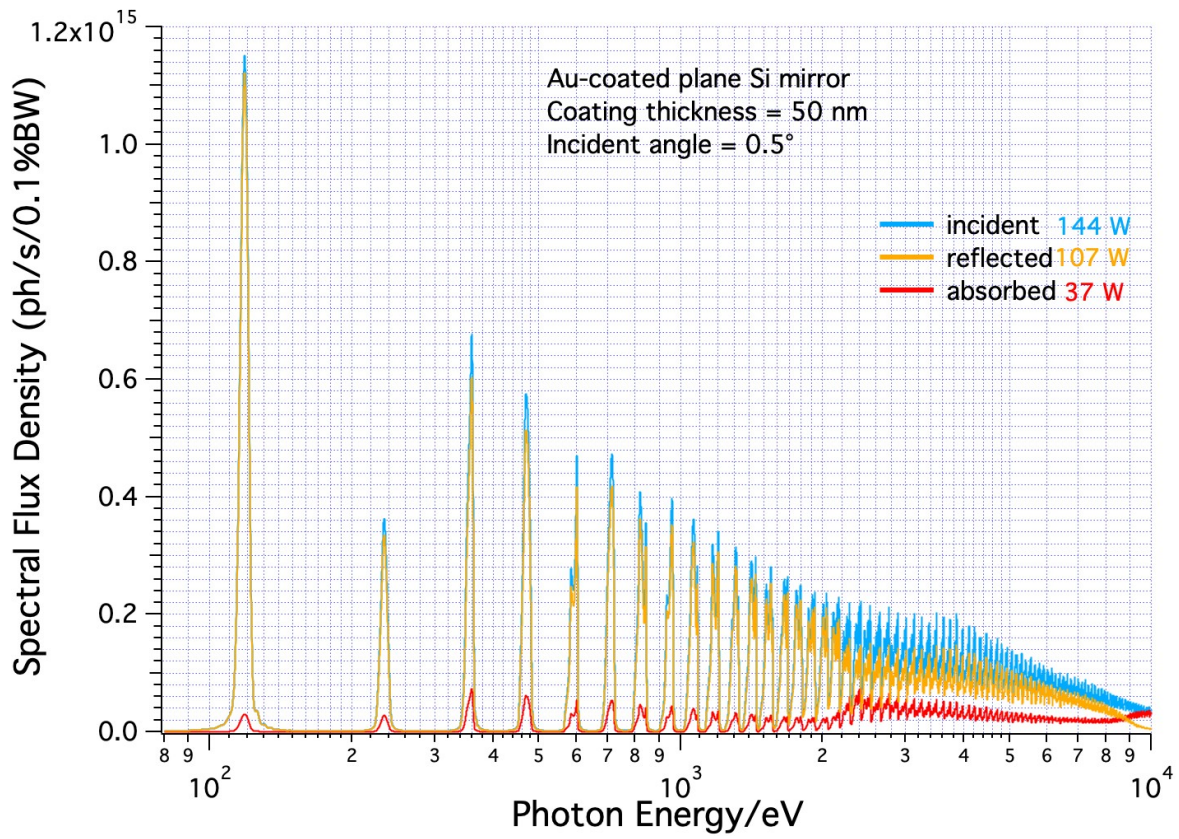


[Figure 22](#). Reflectivity as a function of the photon energy for the incident angles of 0.5° , 0.75° , 1° , 2° and 2.5° , for Au- and Ni-coated Si mirrors. [Back](#) to text

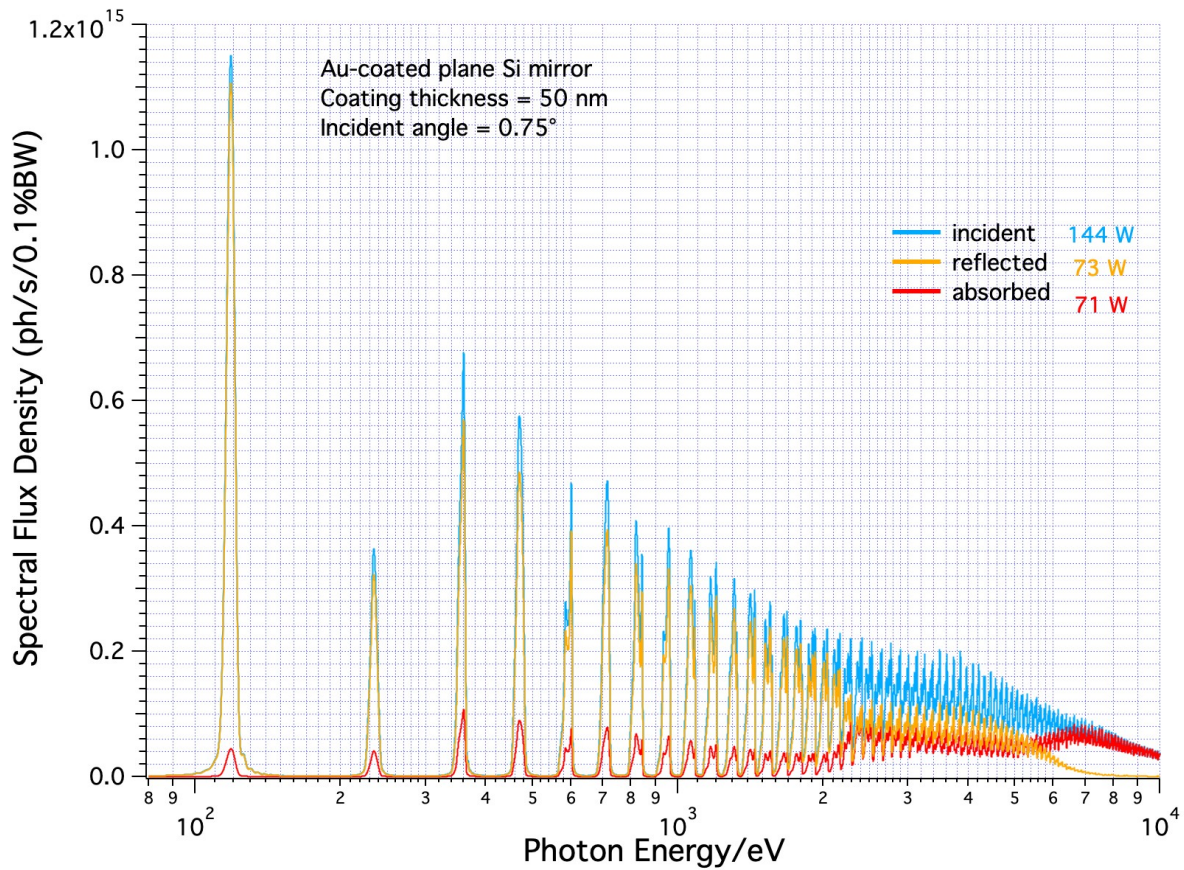
Si mirrors have been taken into account because, as we will see afterwards, these will likely be the materials employed for MOST mirrors. Their reflectivity as a function of the photon energy is displayed in [Fig. 22](#), for the considered angles. Multiplying the SFD on the first mirror for the so-obtained reflectivity curves, and then evaluating integral (3), one can calculate the power reflected and, by subtraction, the power absorbed by the mirror. The results are depicted in Fig. 23 (Au, [0.5°](#), [0.75°](#), [1°](#), [2°](#), [2.5°](#)) and 24 (Ni, [0.5°](#), [0.75°](#), [1°](#), [2°](#), [2.5°](#)) and summarized in Table 10.

Coating	Incidence Angle (°)	Reflected Power (W)	Absorbed Power (W)
Au	0.5	107	37
Ni	0.5	107	37
Au	0.75	73	71
Ni	0.75	72	72
Au	1	51	93
Ni	1	50	94
Au	2	19	125
Ni	2	15	129
Au	2.5	13	131
Ni	2.5	10	134

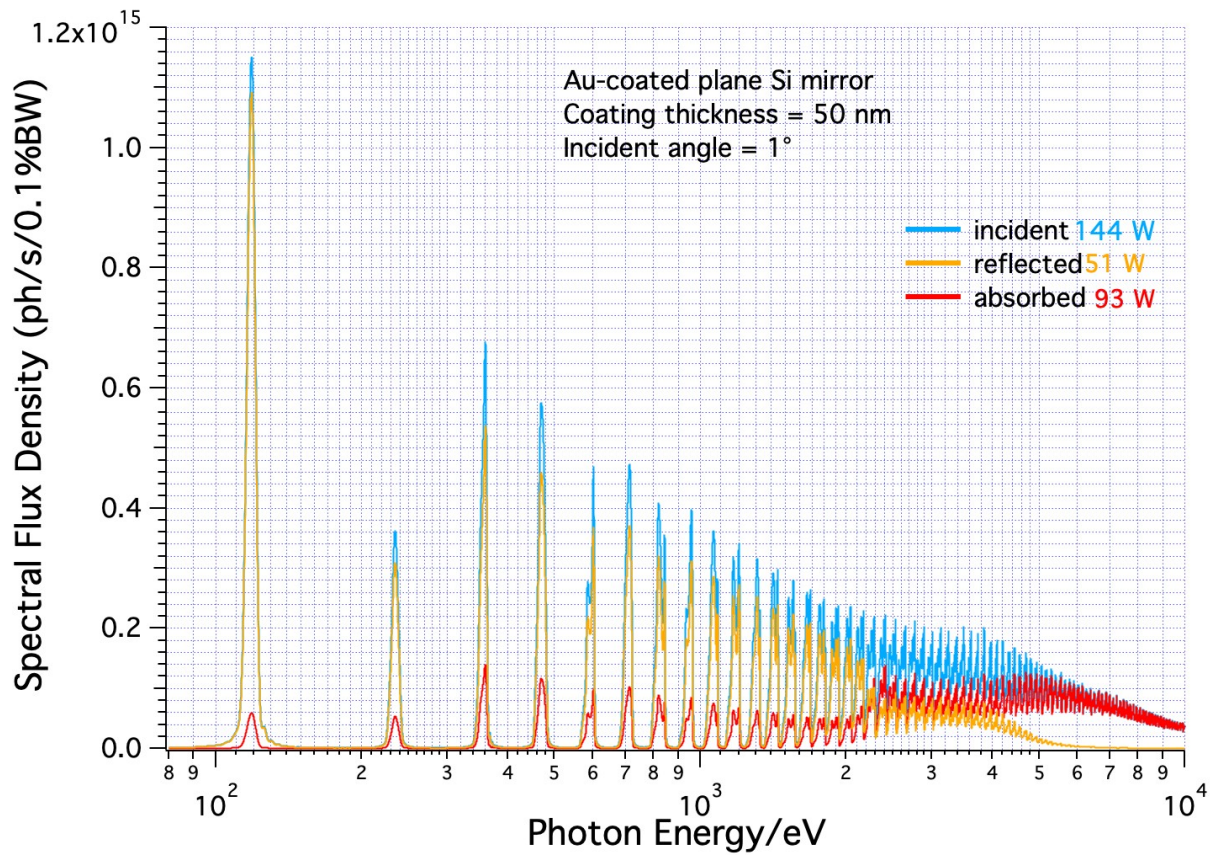
Table 10. Summary of the Reflected Power and Absorbed Power values obtained at different incidence angles for Au- and Ni-coated mirrors.



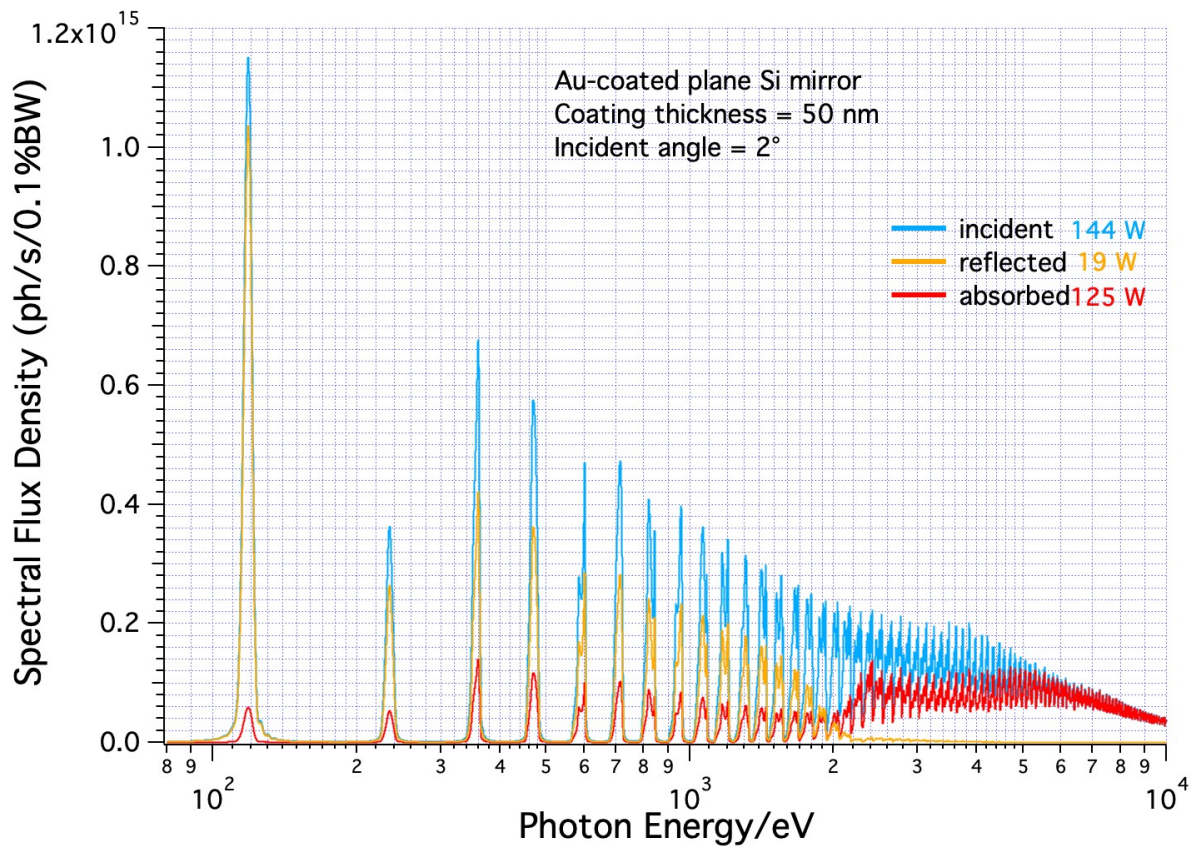
[Back to text](#)



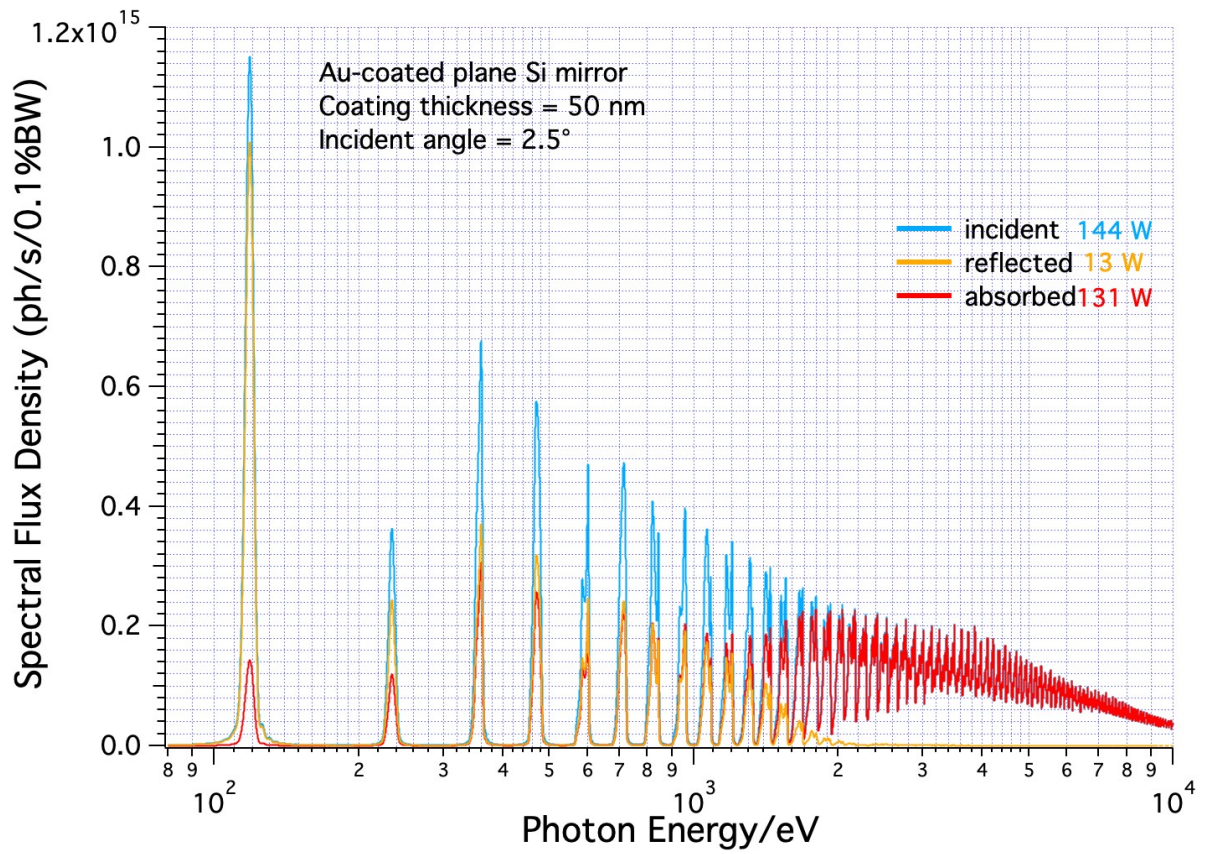
[Back to text](#)



[Back to text](#)

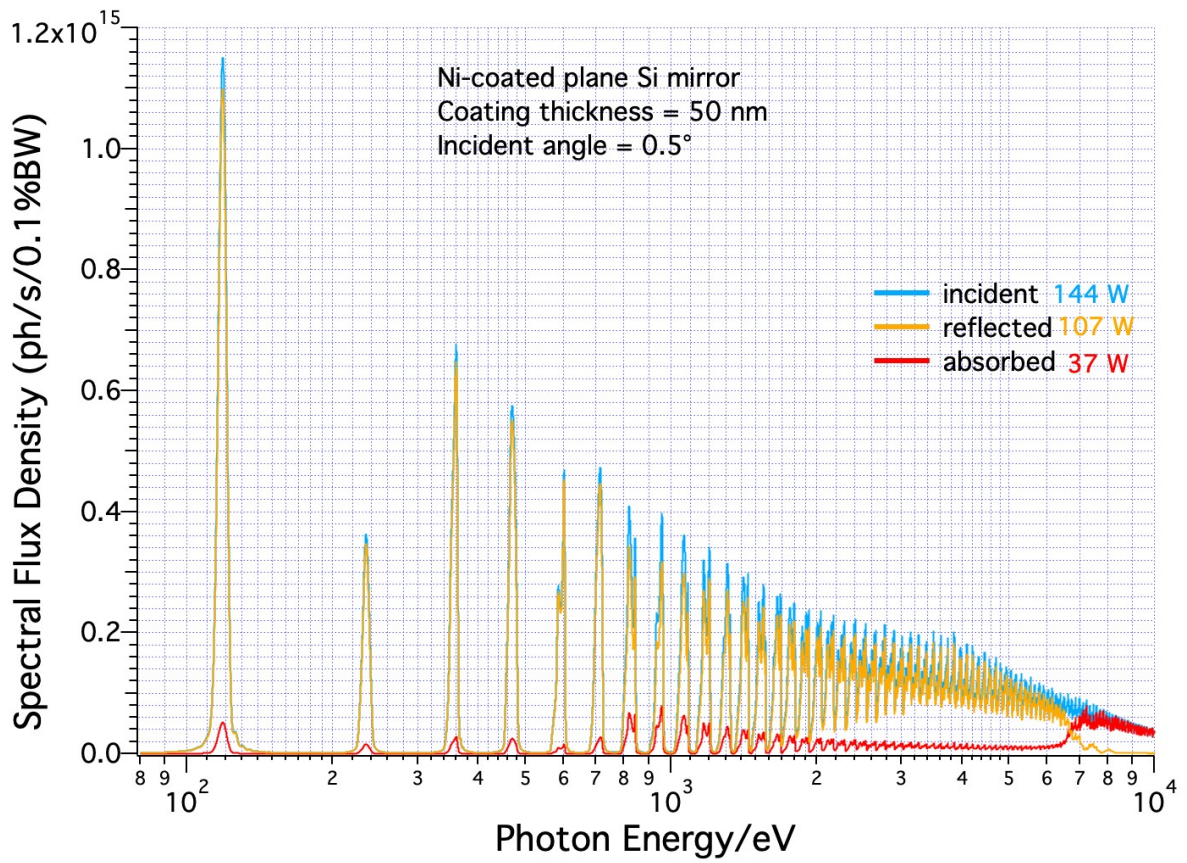


[Back to text](#)

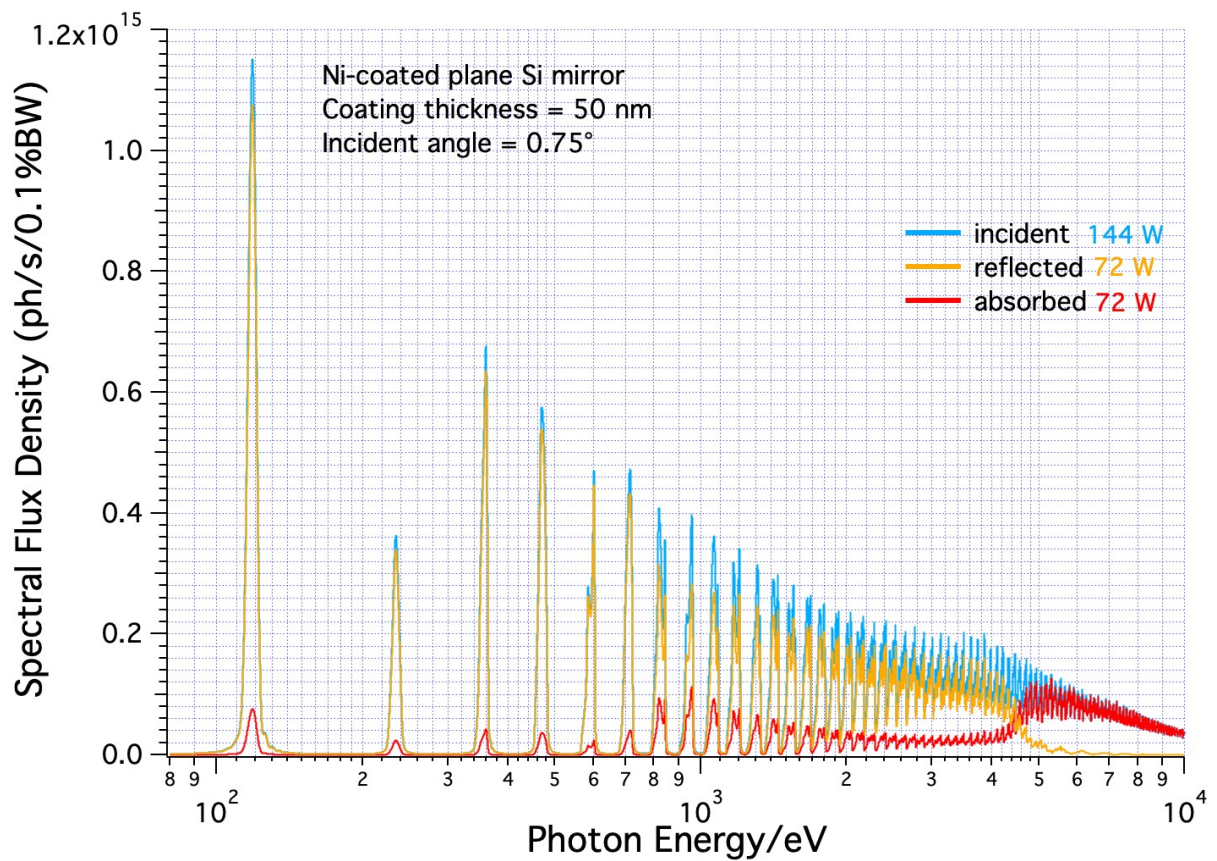


[Back to text](#)

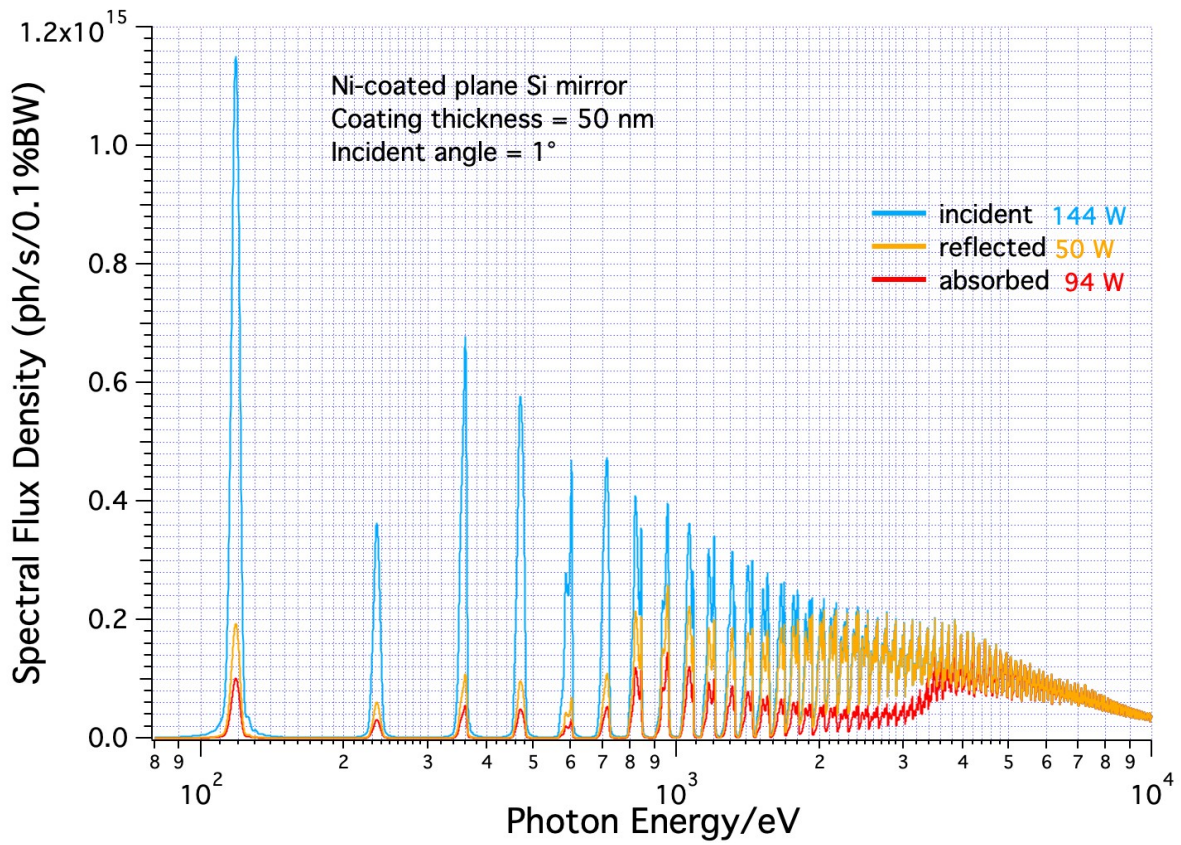
Figure 23. Incident, reflected and absorbed SPF for a Au-coated Si mirror at, from top to bottom, [0.5°](#), [0.75°](#), [1°](#), [2°](#) and [2.5°](#) of incidence of the incoming beam. The incident, reflected and absorbed power values are also indicated.



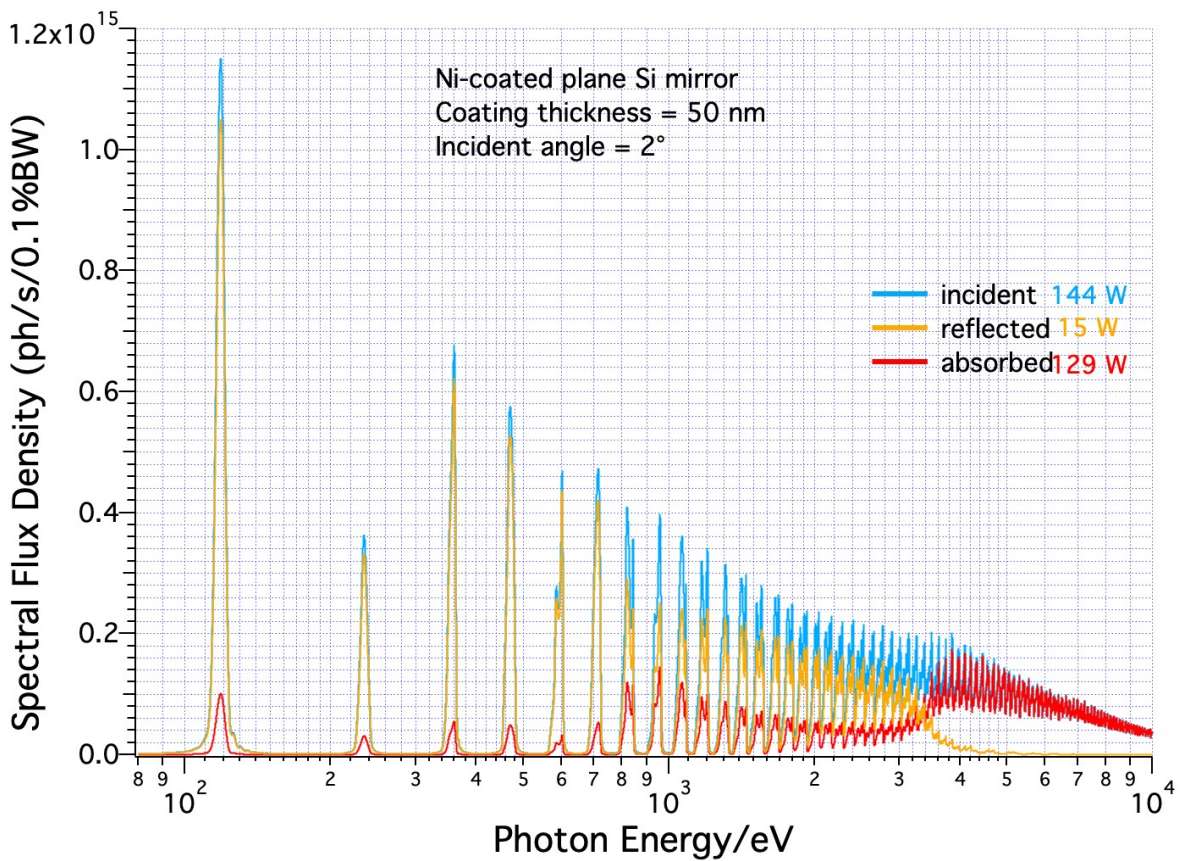
[Back to text](#)



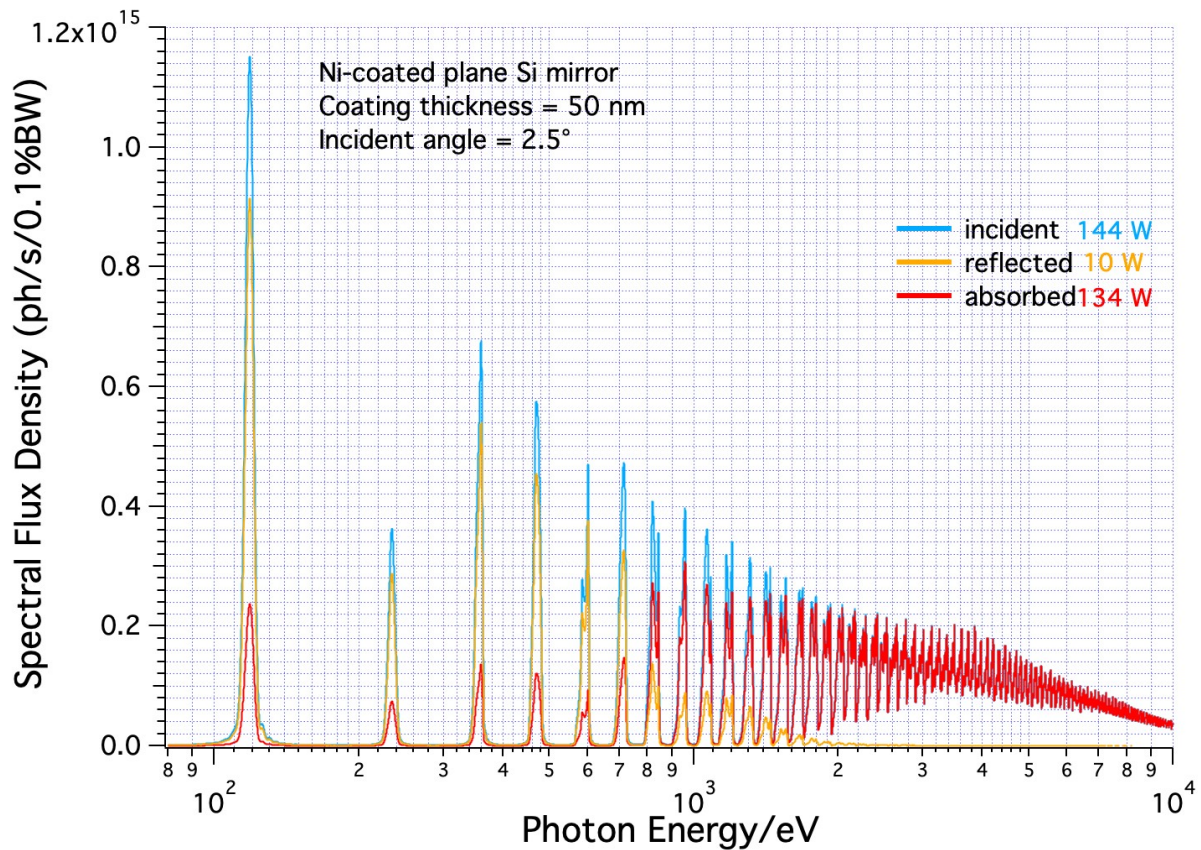
[Back to text](#)



[Back to text](#)



[Back to text](#)



[Back to text](#)

Figure 24. Incident, reflected and absorbed SPF for a Ni-coated Si mirror at, from top to bottom, [0.5°](#), [0.75°](#), [1°](#), [2°](#) and [2.5°](#) of incidence of the incoming beam. The incident, reflected and absorbed power values are also indicated.

These results allowed us to conclude that:

- Extremely grazing incidence angles ($<1^\circ$) are going to be preferred in order to properly deal with the high value of the incidence power and guarantee a proper flux transmission. However this requires very low tangential slope errors on the optical elements, with higher realization costs and constraints on their shape and size.
- Higher incidence angles ($> 1^\circ$) would necessarily require Au-coated mirrors, as Ni (and other commonly used metals) has a drop in reflectivity at photon energies above 2500 eV (see [Fig.22](#)).

4. MOST PRELIMINARY OPTICAL DESIGN - INTERMEDIATE AND HIGH ENERGY

A preliminary design of MOST for intermediate and high photon energies has been recently developed by Luca Poletto and Fabio Frassetto (Istituto di Fotonica e Nanotecnologie, IFN - CNR). Hereafter, the main aspects of the design are reported.

After a survey on the state-of-the-art soft-X-rays beamlines currently operating worldwide, the BOREAS beamline [5] at ALBA synchrotron has been taken as template, as it covers the same photon energy range we are interested in.

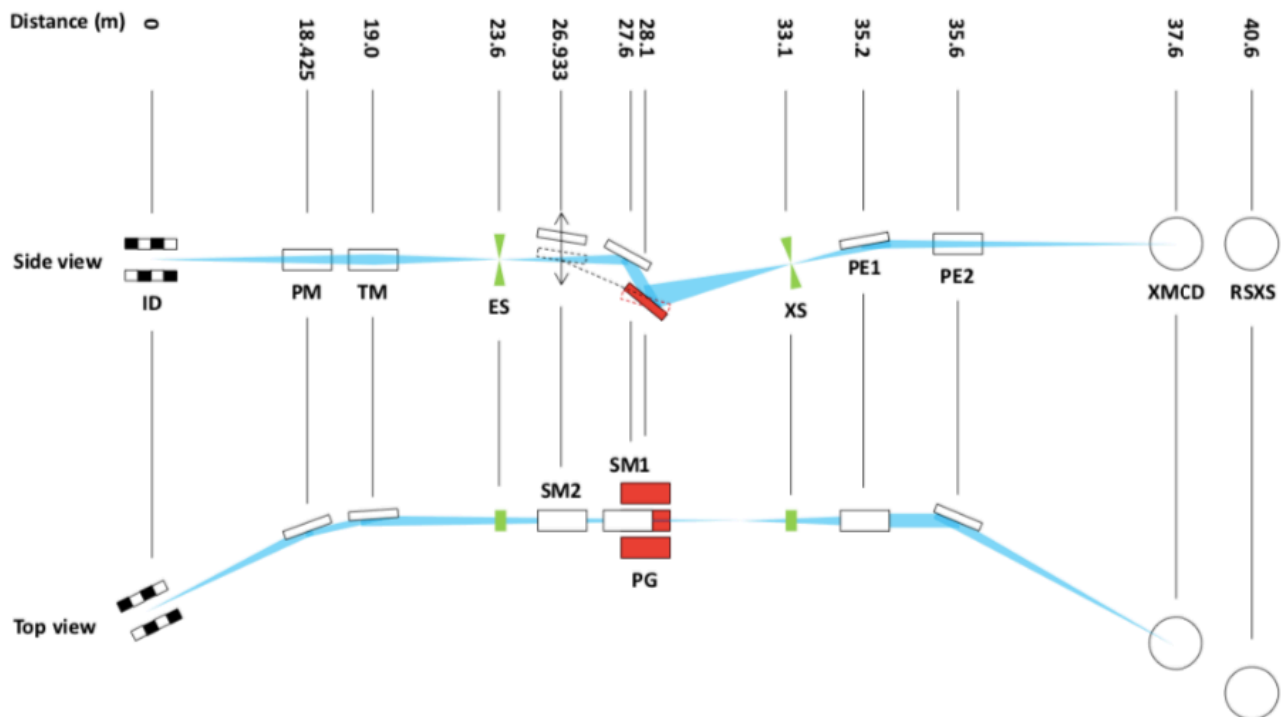


Figure 25. BOREAS beamline optical design [4].

Therefore, for intermediate and high photon energies, MOST will supposedly have a very similar optical design (Fig.25), with the following optical elements:

- **First optical element: PLANE MIRROR (PM).** A plane mirror is required as the first optical element at extreme grazing incidence: 0.75° . This is needed to take care of the high heat load (as seen in the previous paragraph).
- **Pre-focusing: TOROIDAL MIRROR (TM).** Mirror at 89° to have reflectivity up to 3000 eV. The choice of a TM is justified considering that:
 - A tangential focusing on the entrance slit (ES) of the monochromator is to be avoided, since it would require very low tangential slope errors on the mirror surface \rightarrow no KB system.
 - A stigmatic focusing on ES is to be avoided, for the high thermal load that could damage the slit surface \rightarrow no ellipsoidal mirror.

Therefore, an astigmatic focusing is to be adopted, i.e. a sagittal focusing on the ES plane in the vertical direction (perpendicular to the slit) and a tangential focusing after the ES plane in the horizontal direction, in order to limit the peak intensity on the ES plan. This is possible by employing a TM. Note that the astigmatic focus is aberrated in the direction parallel to the slit (hourglass shape), thus ES has to be kept quite wide to give the highest transmission

- **Monochromator: SPHERICAL MIRRORS (SM) + PLANE GRATINGS (PG)**

- The PGs will have a Variable Line Spacing (VLS) configuration: the energy scanning will be achieved with grating rotation.

- The geometry choice of these elements is explained considering that they will need very low tangential slope errors to achieve high photon energy resolution (at least <0.4 , ideally $<0.2 \mu\text{rad rms}$) and spherical and plane optics are most suitable for high surface quality.

- The Monochromator will provide a demagnification factor to the beam size: with an exit/entrance arm and an anamorphic factor (depending on energy).

- The highest resolution will be obtained with the exit slit (XS) closed at $10 \mu\text{m}$, while ES will be open as a function of the energy, ranging from $20 \mu\text{m}$ to $60 \mu\text{m}$, up to the largest value that does not degrade the resolution

- **Focusing: TOROIDAL MIRROR VS. CYLINDRICAL MIRRORS IN KB CONFIGURATION.**

At this point of the beamline there will be two sources: a vertical source on the XS plane and a horizontal source between the two slits. Two options are available for the focusing optics:

OPTION 1

- Single toroidal mirror at 89° to provide a stigmatic focus

- Output beam not parallel to the floor, 2.5° inclination
- 3 m mirror arms are needed, to achieve a feasible sagittal radius (>50 mm) at 89°
- Focus size: 90 μm FWHM X 50 μm FWHM @ 83 eV, 45 μm FWHM X 30 μm FWHM @100 eV, smaller at higher energies

OPTION 2

- KB focusing with two spherical mirrors, one at 89° and one at 89.25°
- Output beam not parallel to the floor, 0.5° inclination (this geometry maximizes the flux in the 2-3 keV range)
- Cylindrical mirrors with two coated stripes are preferable to maximize the flux above 2 keV (with two stripes over 2 mirrors, e.g. Au and Pd/Ni, an increase of a factor 2.5 in the flux is expected). Both cylindrical mirrors have to be translated
- Focus size: 35 μm FWHM X 25 μm FWHM @ 83 eV, 25 μm FWHM X 20 μm FWHM @100 eV, smaller at higher energies.

It is important considering that:

- Although the first plane mirror could be translated to optimize the throughput over 2200 eV, it is preferable to have the mirror with a single coating (Au), to avoid translations of optical elements before the monochromator, that could influence the alignment/calibration of the monochromator. If a single coating has to be chosen, the only feasible option is Au because, as discussed in the previous paragraph, an abrupt drop in reflectivity characterizes all other commonly used metals for photon energies higher than 2500 eV. However, the double coating can be implemented after the monochromator. In case of KB option (option 2) for the focusing optics, the cylindrical mirrors can be designed by adding a second Ni stripe to optimize the throughput for energies above 2200 eV, where the Au reflectivity drops.

- If measurements above 3000 eV are requested, Pd cannot be used (L3 edge at 3170 eV, reflectivity cut-off) and Cr reflectivity is decreasing faster than Au. Ni is eventually the only viable option compared to Au.

- Design parameters

Plane Mirror	18 m from the source, 0.75°, 400 mm long
Toroidal Mirror	19 m from the source, 1°, 300 mm long
Entrance Slit	25 m from the source
Monochromator : Spherical Mirrors	3 mirrors: 3.25°, 1.5°, 0.75°, 160 mm long
Monochromator: VLS Plane Gratings	6.2 m from ES. Three gratings, 200 mm long: - 600 gr/mm, 171° - 1200 gr/mm, 174.5° - 1800 gr/mm, 176°
Exit Slit	4 m from the gratings
Focusing Mirror - Option 1	KB: 2 cylindrical mirrors, focal distance 2 m Mirror 1: 0.75°, mirror length 300 mm Mirror 2: 1°, mirror length 400 mm
Focusing Mirror - Option 2	Single-mirror: toroidal mirror, focal distance 3 m Mirror: 1°, mirror length 250 mm
Beamline Length	Focal point: 38.2 m from the source Focal point: 41.2 m from the source

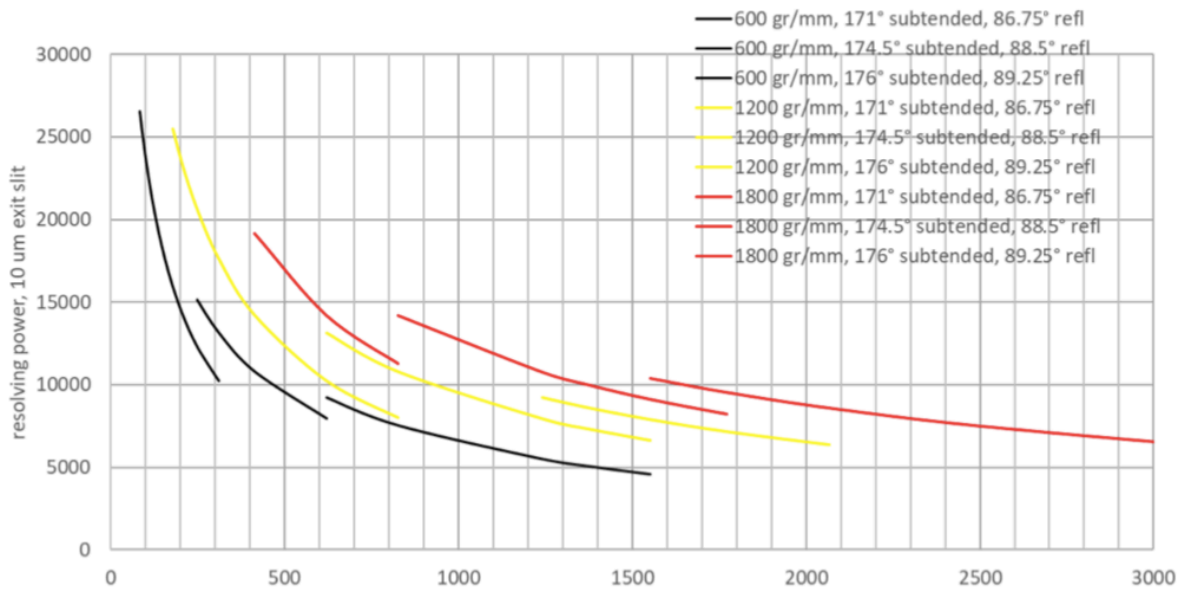


Figure 26. Gratings resolving power for different subtended angles, as a function of the photon energy.

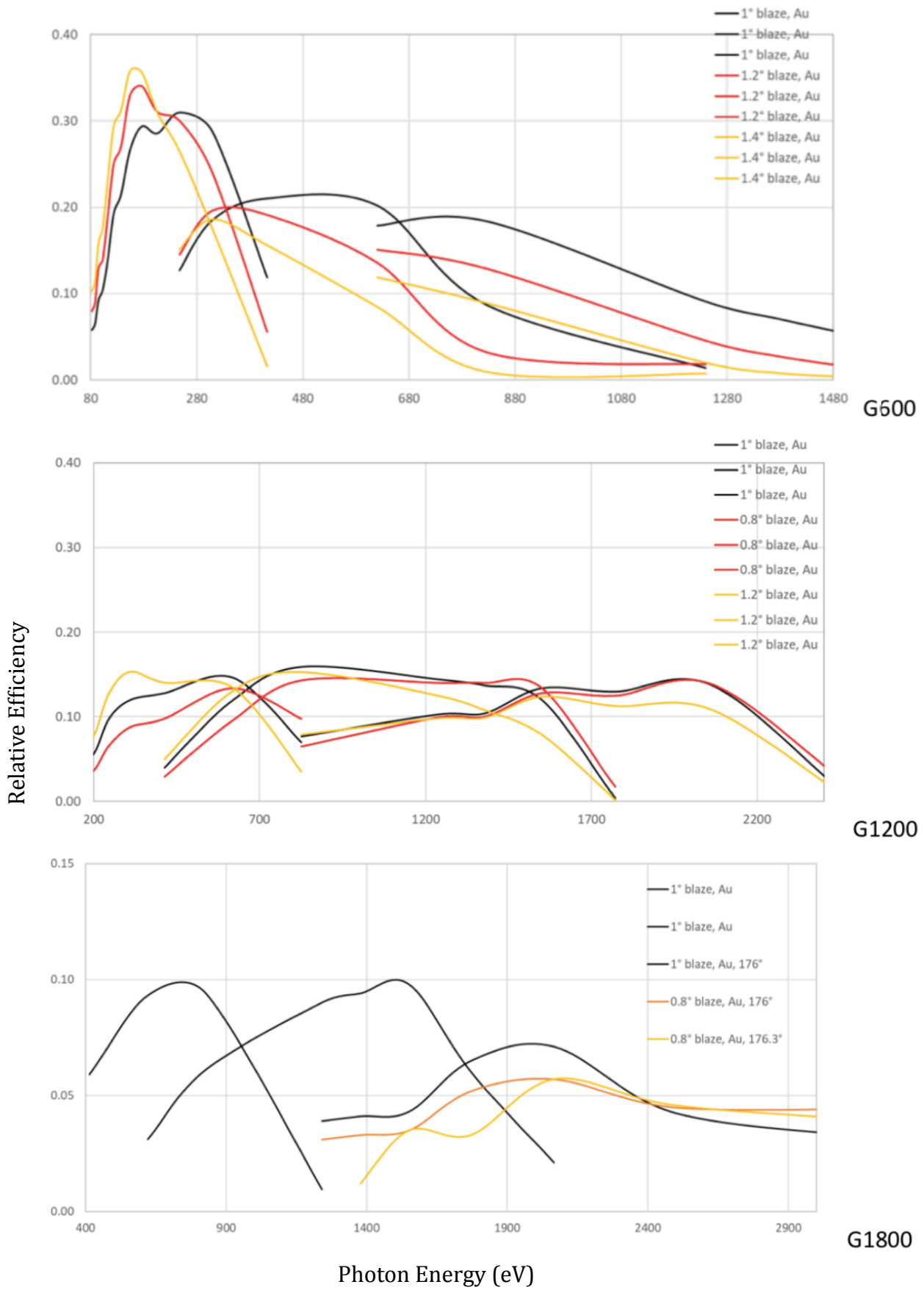


Figure 27. Gratings efficiency, for the three gratings and for different blaze angles, as a function of the photon energy.

5. MOST BEAMLINE: A STEP-BY-STEP REALIZATION

MOST realization will occur in two distinct phases:

- MOST 1, before ELETTRA 2.0 (until December 2025)
- MOST 2, after ELETTRA 2.0 (starting from January 2026).

During MOST 1, GasPhase will be kept operative, while the main changes will be realized at CiPo. Here the new undulators will be installed and will start working with the old CiPo monochromator, after the update and the refurbishment of the NIM (Normal Incidence Monochromator) for low photon energies (8, 10 eV - 35 eV). The grazing incidence monochromator (SGM) for medium and high energies (35 eV - 1000 eV) will not be modified. After the shutdown, the GasPhase monochromator will be relocated to the new MOST beamline, entering its phase 2. The LEU, together with CiPo NIM and the GasPhase monochromator (SGM), will cover the low and medium photon energy range: from 8,10 eV to 35 eV with the NIM and from 25 eV to 600 eV with the SGM, as depicted in the schematic layout of [Fig.28](#).

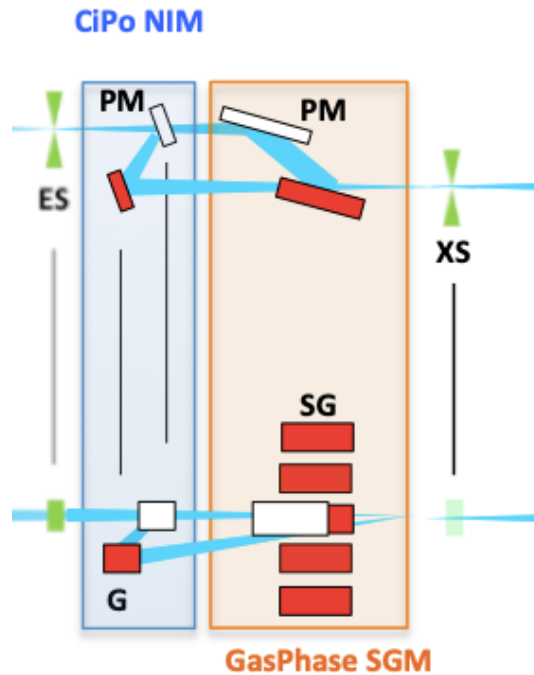


Figure 28. Low- and medium-energy MOST monochromator, realized by employing the CiPo NIM and the GasPhase SGM.

Meanwhile, the high-energy design will be completed and, supposedly, the new optical elements (described in the previous section) delivered, so that their installation will be able to start latest by the beginning of the shutdown. The HEU, together with the new optical elements will cover the high-energy range, from 80 eV to, presumably, 3000 eV.

The configuration of the insertion devices (in line or canted) is still under debate. The “in line” configuration will greatly facilitate the optical layout design, necessitating less space and a smaller number of optical elements. Besides, MOST is going to operate alternatively at low/medium energies or high energies, with a lower effort in terms of workforce. However, the canted configuration, originating two different branches, will allow the contemporary operation in the two photon-energy ranges. This will double the available shifts and the feasible experiments but also the staff required to run both branches at the same time. Further discussions will be needed to clarify this issue.

REFERENCES

- [1] B. Diviacco, MOST Workshop, Trieste, 20-21 January 2020
- [2] Parameters validated by B. Diviacco, October 2020
- [3] <http://spectrax.org/spectra/>
- [4] Insertion Devices: Undulators and Wigglers, R. P. Walker, Invited lectures at the CERN Accelerator School on Synchrotron Radiation and FEL. Grenoble, April 1996.
- [5] Barla et al., *J. Synchr. Rad.* **23** (2016), 1507-1517